Evidence for $H \rightarrow \mu^+ \mu^-$ in pp collisions with the ATLAS detector

Ehsan Musajan
University of Science and Technology of China

The 11th China LHC Physics Conference
新乡, October 30, 2025

Introduction

- In the Standard Model, all known elementary particles acquire mass through the **BEH mechanism** responsible for the Electroweak Symmetry Breaking
- Fermions, in particular, acquire mass through **Yukawa interactions** with the Higgs boson
- ATLAS and CMS observed Higgs boson couplings to third-generation fermions

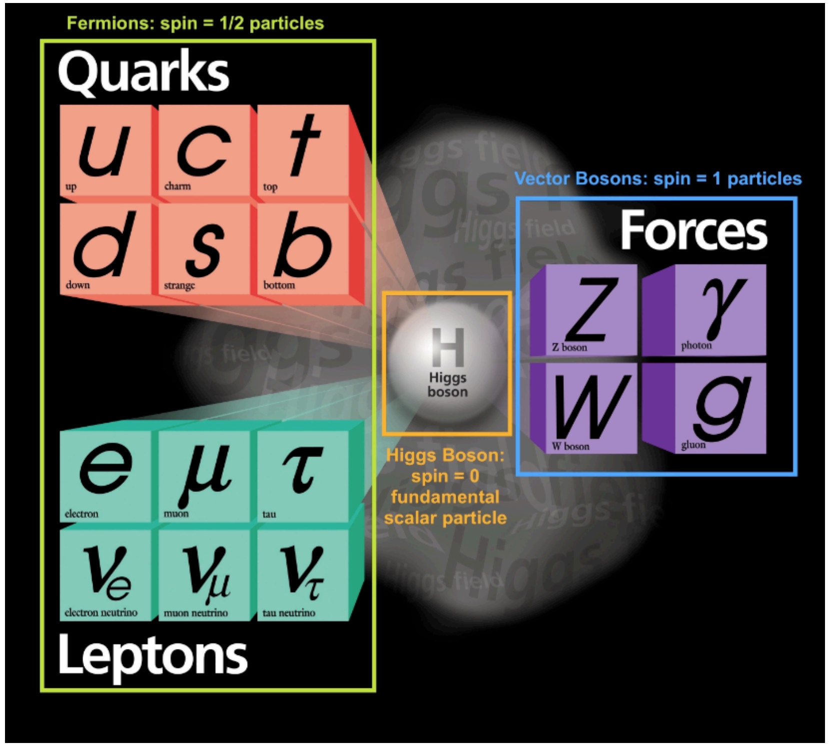

$H\to\tau\tau$

Observation at 6.4σ

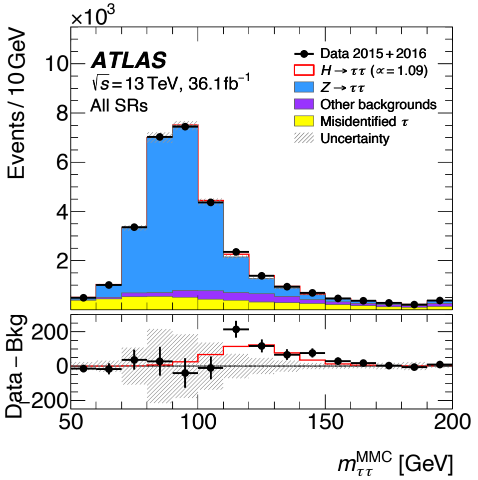

[Phys. Rev. D 99 (2019) 072001]

ttH

Observation at 5.8σ

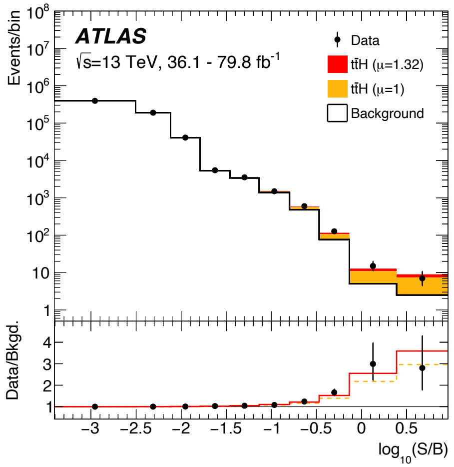

[Phys. Lett. B 784 (2018) 173]

$H\to bb$

Observation at 5.4σ

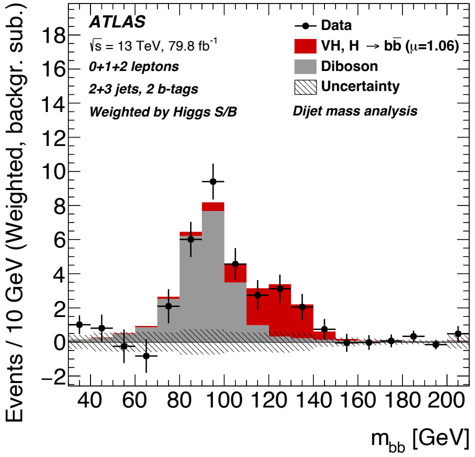

[Phys. Lett. B 786 (2018) 59]

Introduction

- Next milestone: search for couplings to second generation fermions.
- **H→μ+μ-** offers the best opportunity to accomplish this at the LHC!
- Previous analyses:
  - ATLAS: [Phys. Lett. B, 812 (2021) 135980](), obs.(exp.) significance $2.0\sigma(1.7\sigma)$
  - CMS: [JHEP 01 (2021) 148](), obs.(exp.) significance **3.0σ**(2.5σ), **evidence**

[Nature 607 52 (2022)]()

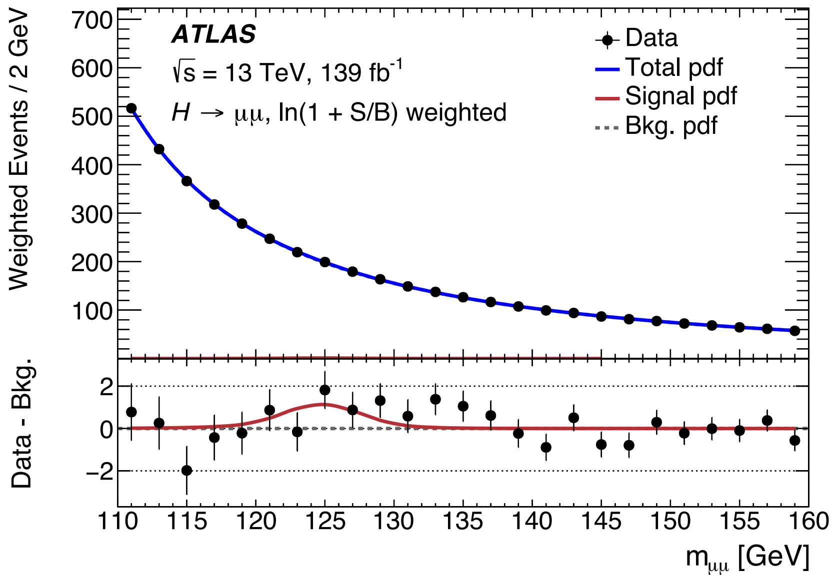

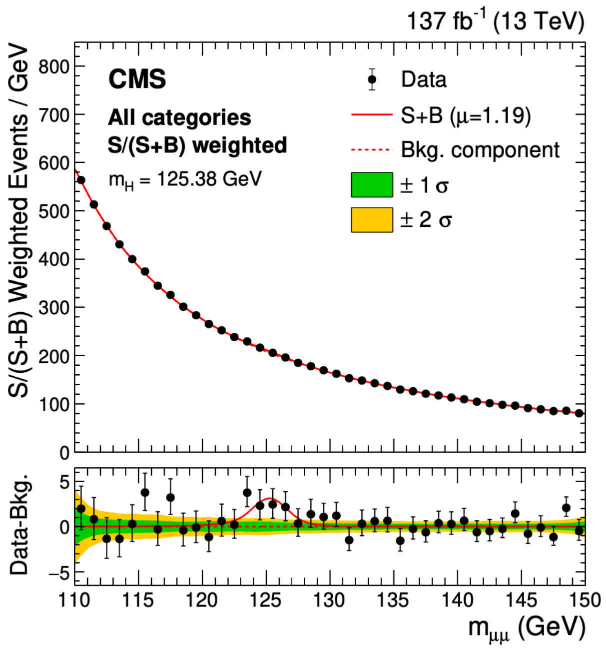

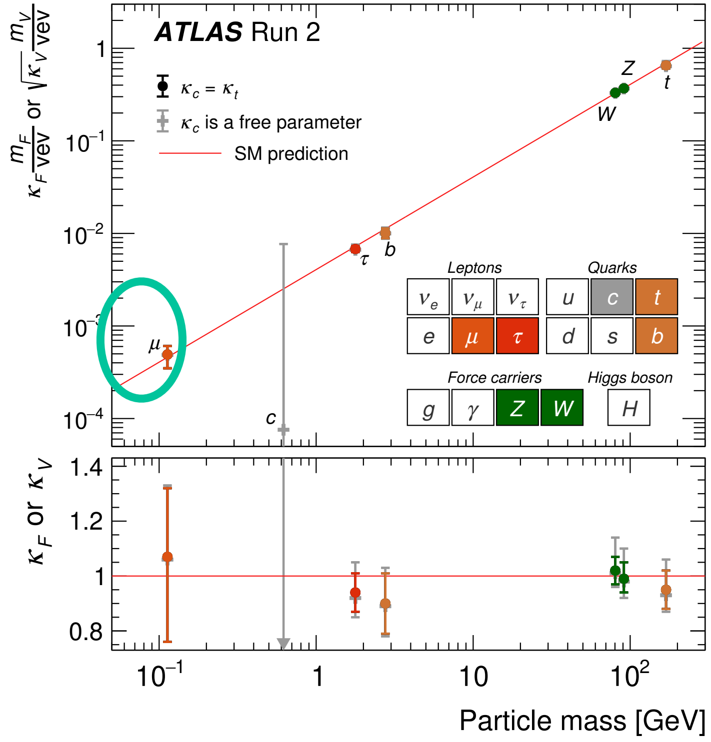

◉ Run 3: new result from ATLAS!

Challenge

- Very small signal/background ratio, **typically O(0.1%)**
  - **Rare process**: branching ratio of $(2.17 \pm 0.04) \times 10^{-4}$
    - If compared to the third generation: $BR_{H\to\mu\mu}/BR_{H\to\tau\tau} \sim (m_\mu/m_\tau)^2 = 0.35\%$
  - **Large background** from Drell-Yan $\mu^+\mu^-$ production
    - Compared with the $H\to ZZ\to 4l$ with even smaller BR and but much smaller background.

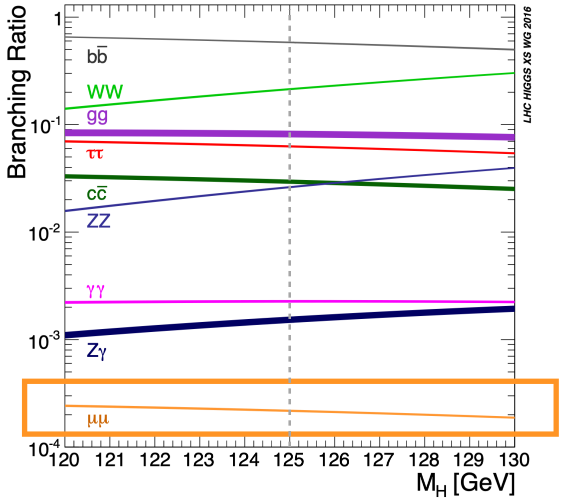

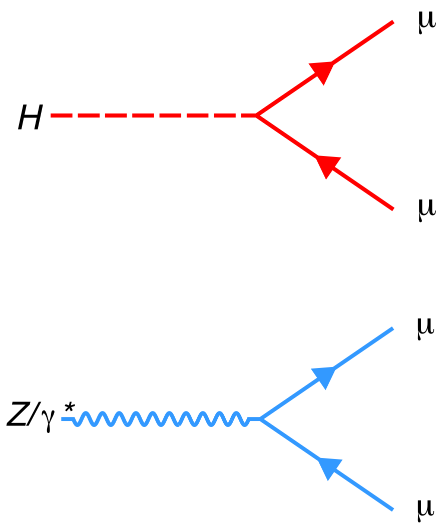

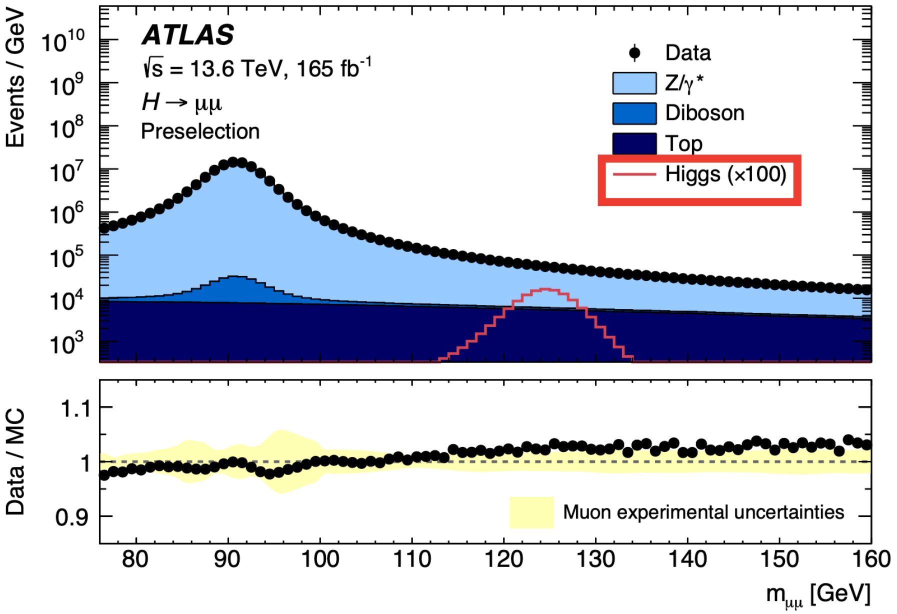

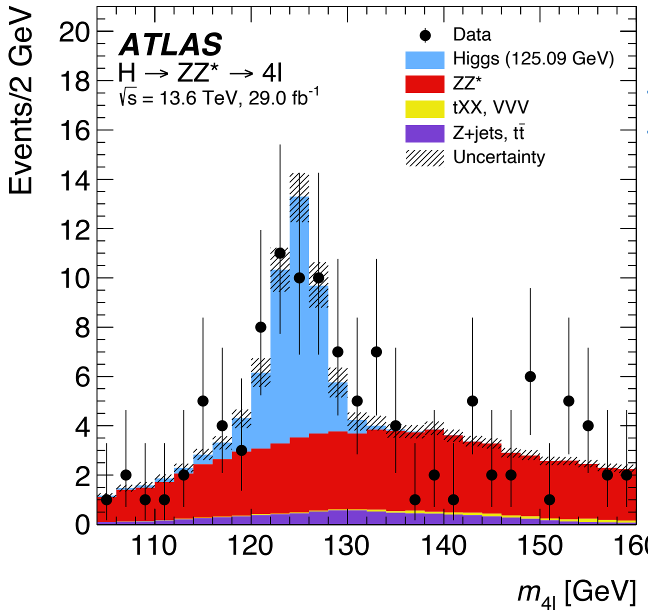

Eur. Phys. J. C 84 (2024) 78

Keys to search for H→ μ+μ- signal

- **Large dataset**, thanks to the LHC!
- **Excellent muon reconstruction performance**
- **Machine learning to suppress background**
- **Accurate background modeling**

ATLAS luminosity

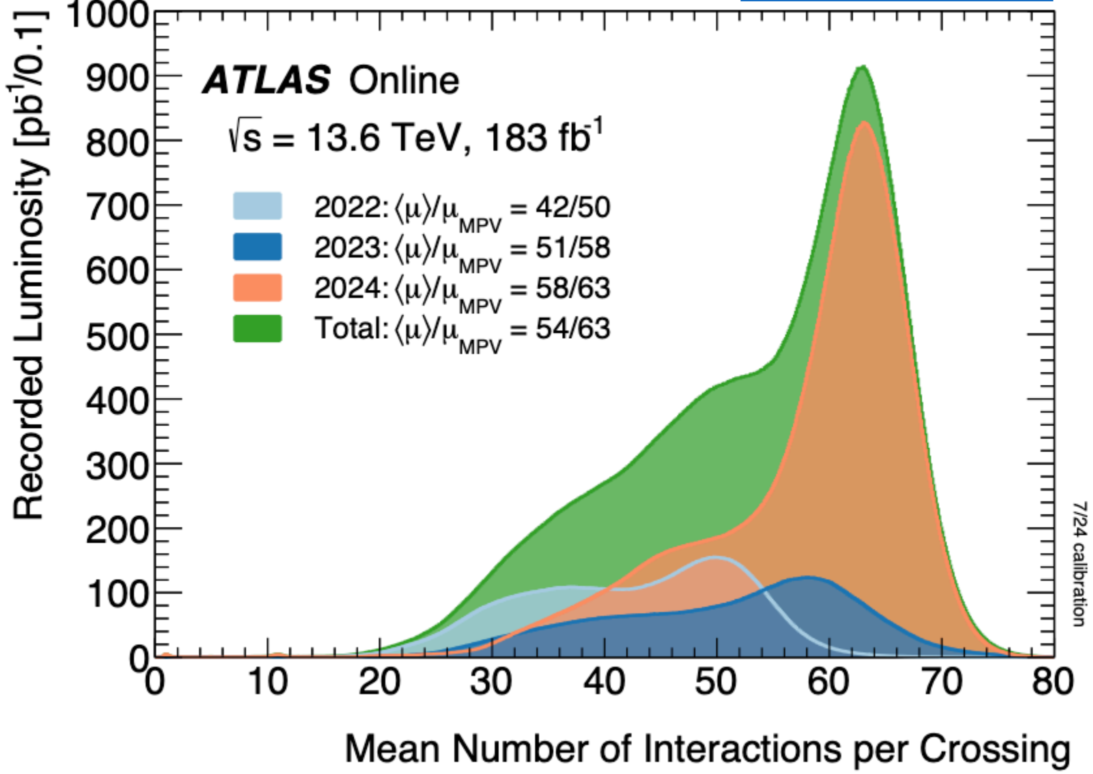

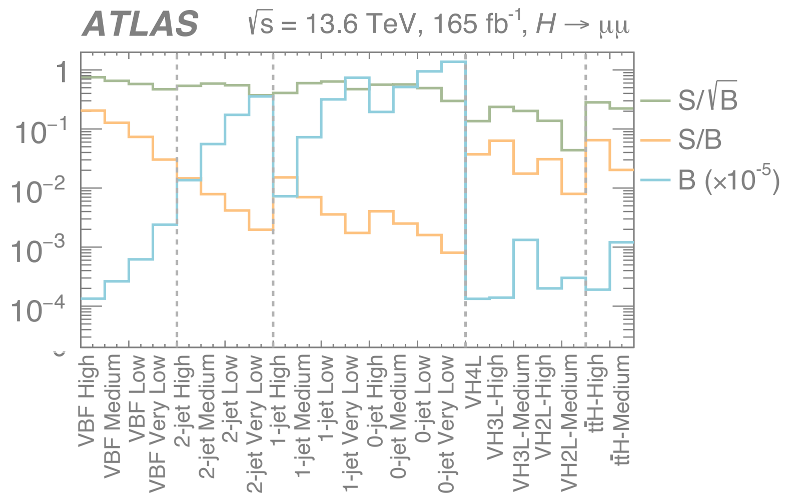

Analysis categories

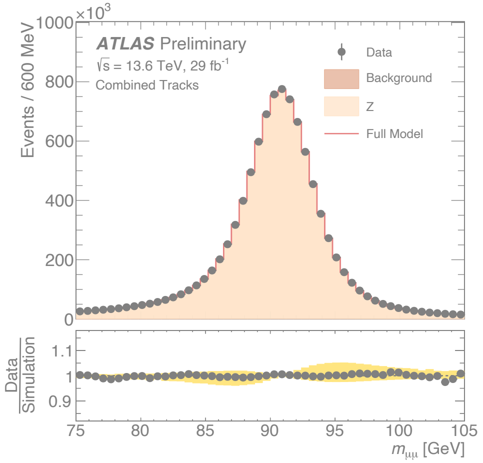

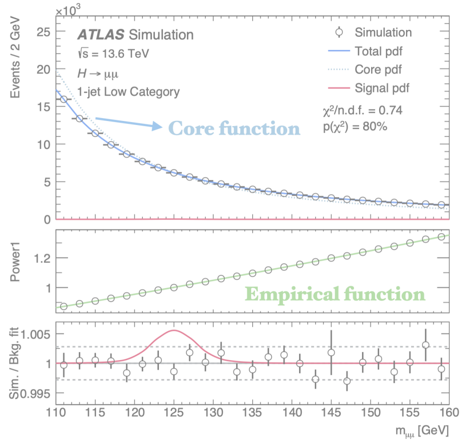

Keys to search for H→ μ+μ- signal

- Large dataset, thanks to the LHC!
- **Excellent muon reconstruction performance**
- Machine learning to suppress background
- Accurate background modeling

MUON-2023-02

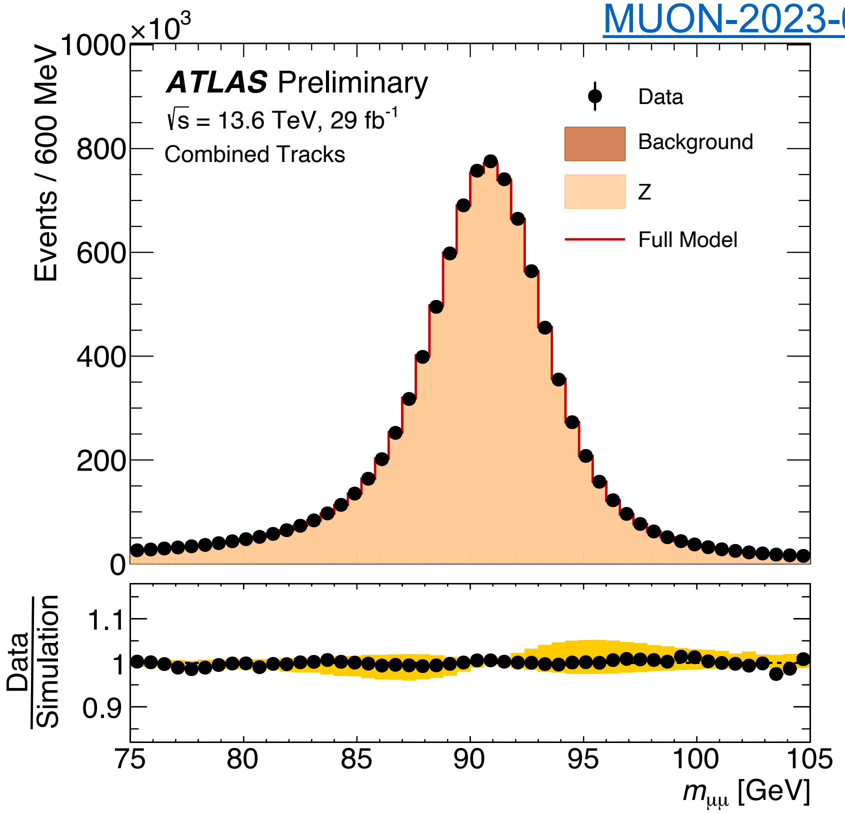

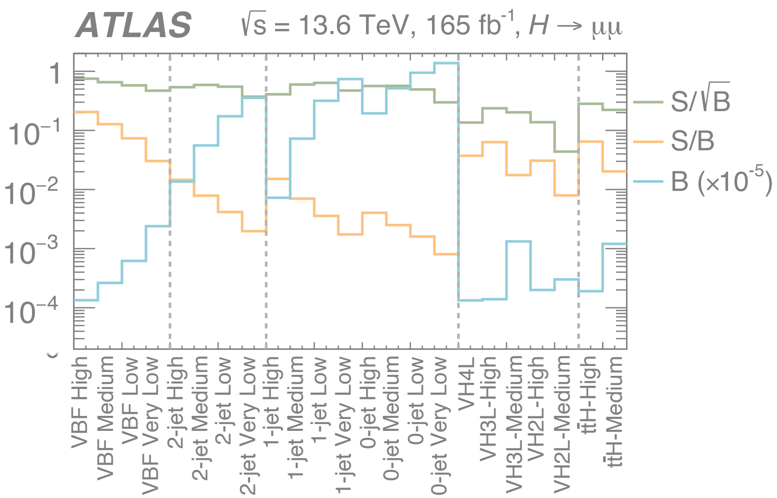

Analysis categories

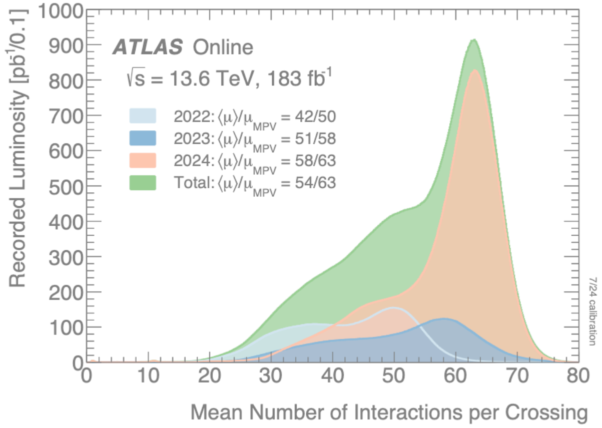

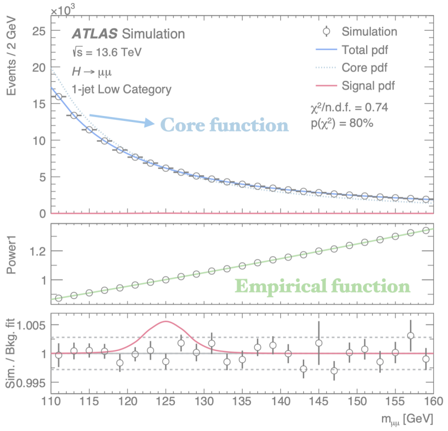

Keys to search for H→ μ+μ- signal

- **Large dataset**, thanks to the LHC!
- **Excellent muon reconstruction performance**
- **Machine learning to suppress background**
- **Accurate background modeling**

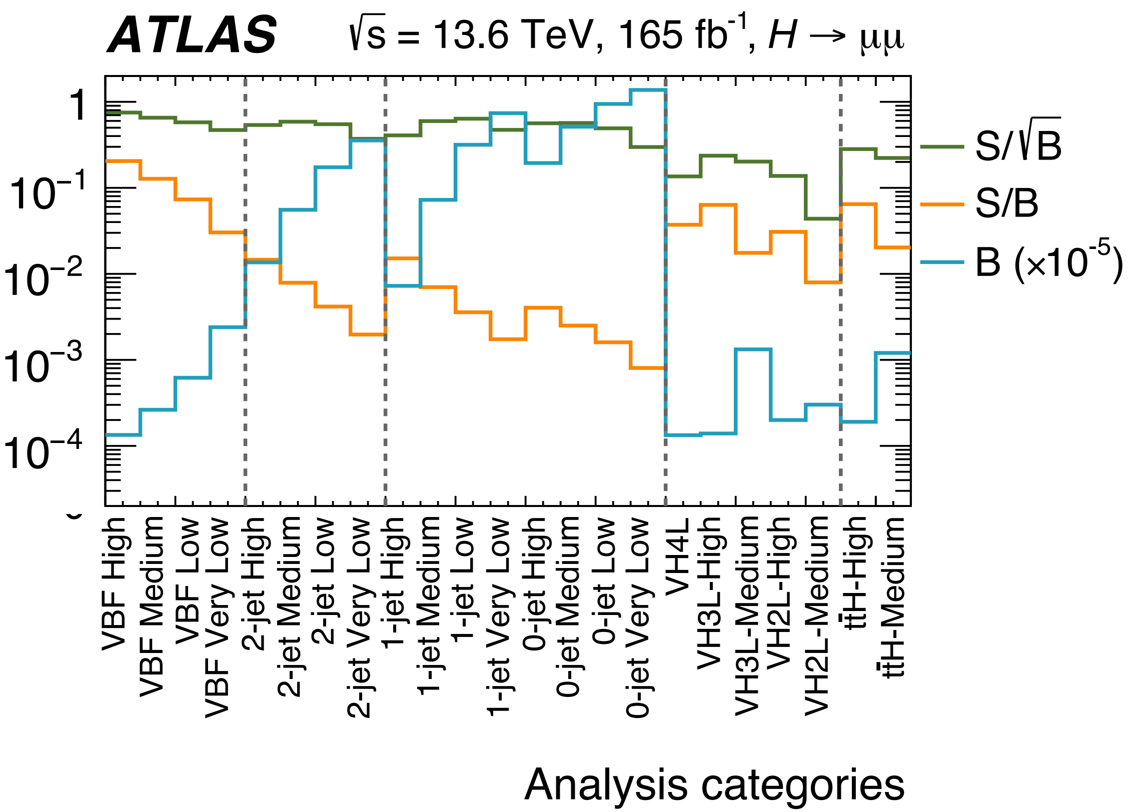

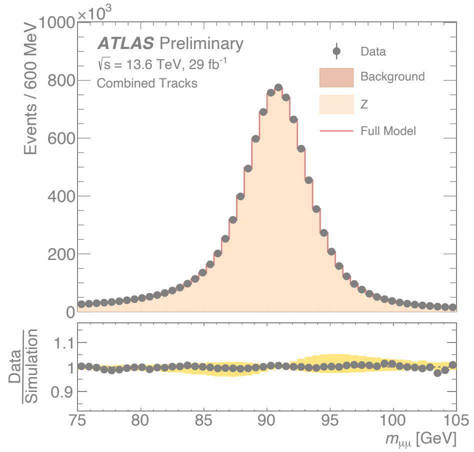

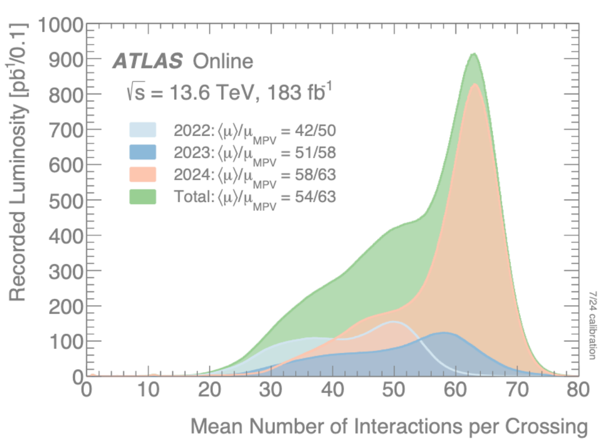

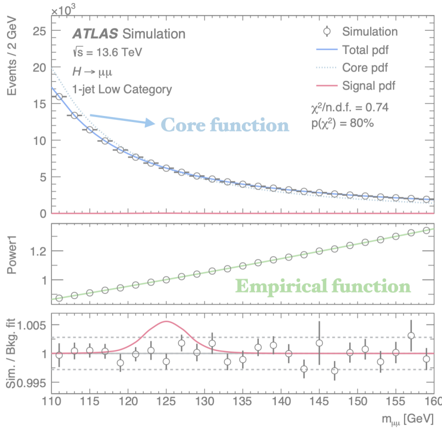

Keys to search for H→ μ+μ- signal

- **Large dataset**, thanks to the LHC!
- **Excellent muon reconstruction performance**
- **Machine learning to suppress background**
- **Accurate background modeling**

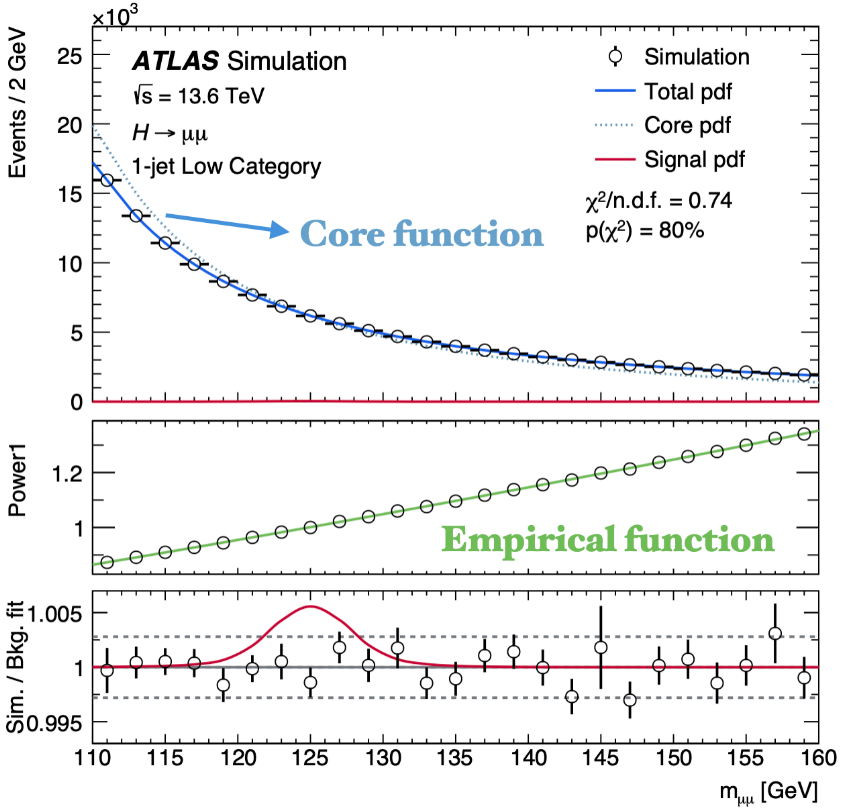

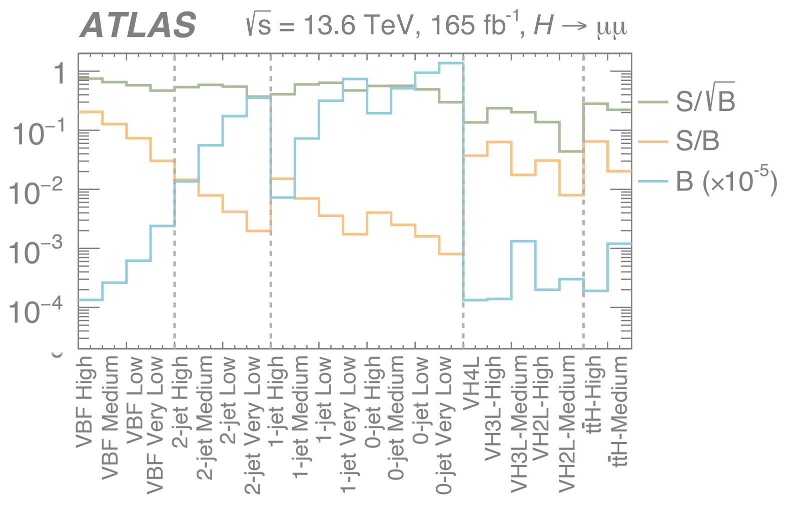

Analysis categories

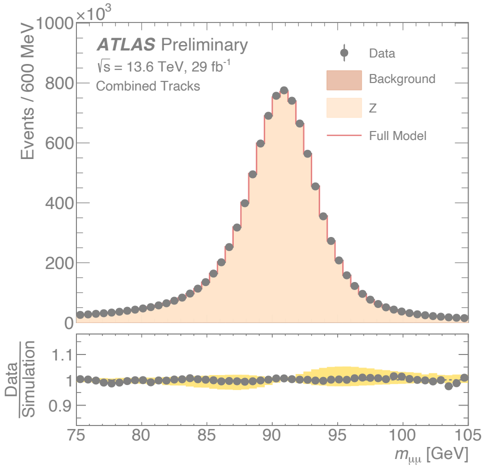

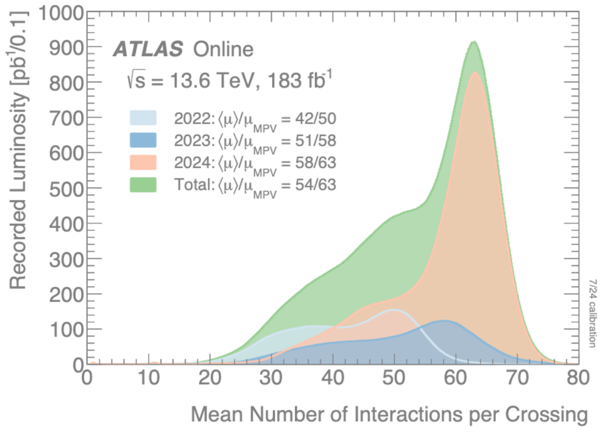

Partial Run3 dataset (2022~2024)

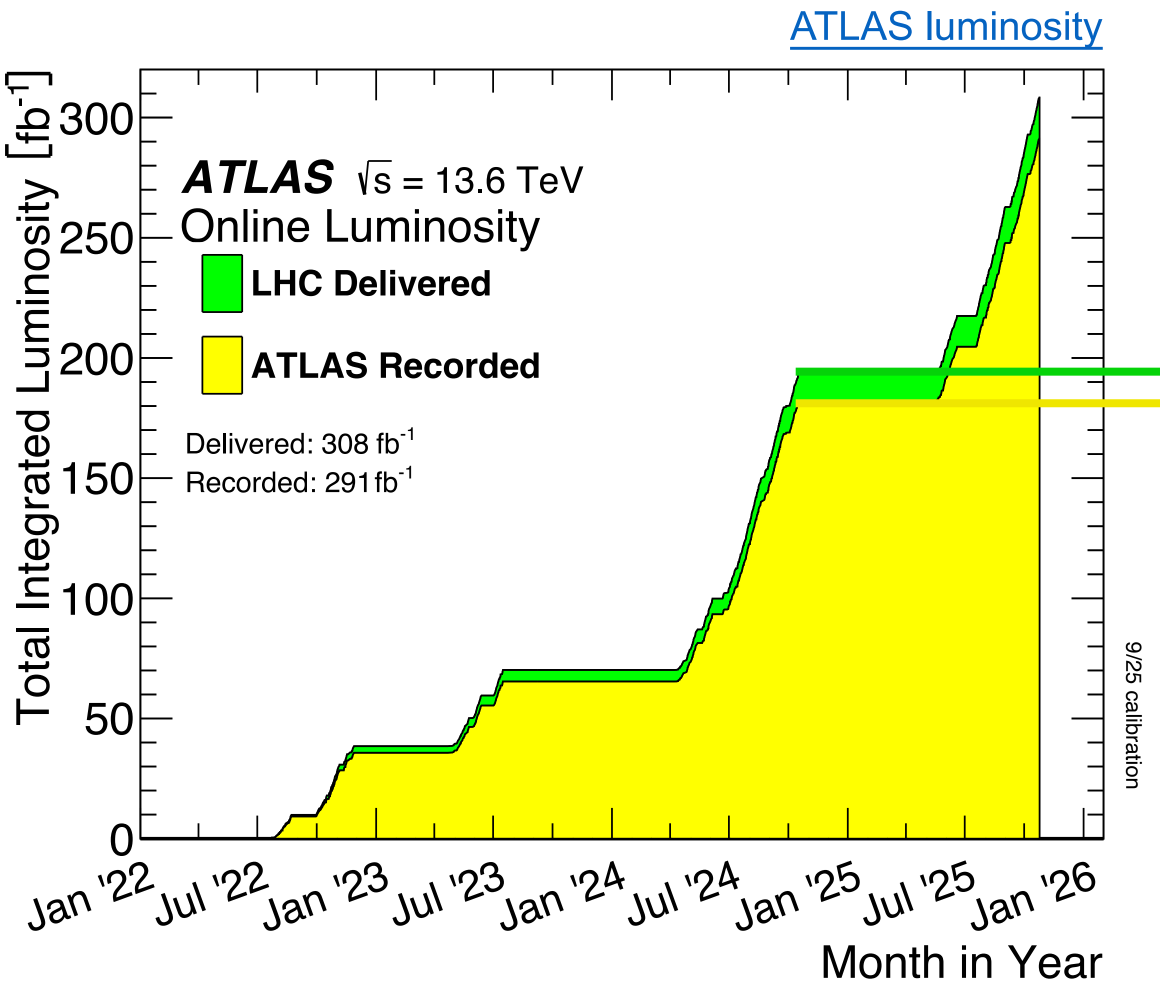

- Successful **Run 3** pp collision data taking at $\sqrt{s} = 13.6$ TeV by ATLAS!
  - Delivered by the LHC: 195 fb^{-1} (by end of 2024)
  - Recorded by ATLAS: 183 fb^{-1}
  - Good for Physics: **165 fb^{-1}**
- **+ 140 fb^{-1}** @13 TeV from **Run 2**

Muon reconstruction and calibration

- Muon calibrations have been updated using Run 3 dataset, up to 165 fb^{-1} total luminosity.
- High efficiency for muon reconstruction, identification (top left), and isolation (top right).

MUON-2023-02

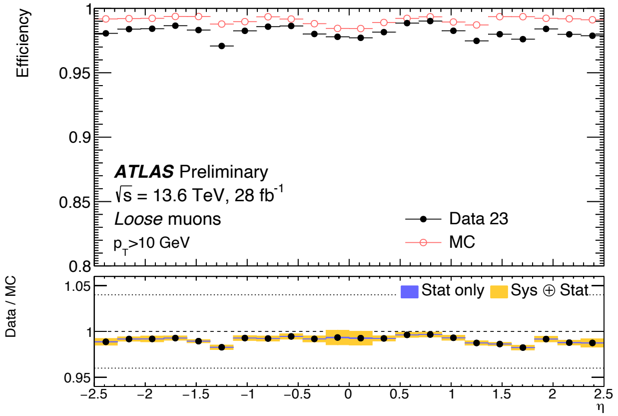

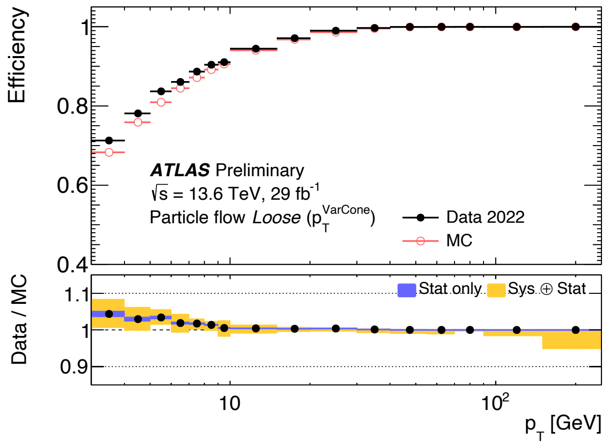

- Well modeled by simulation, and calibrated using J/ψ and Z as candles.

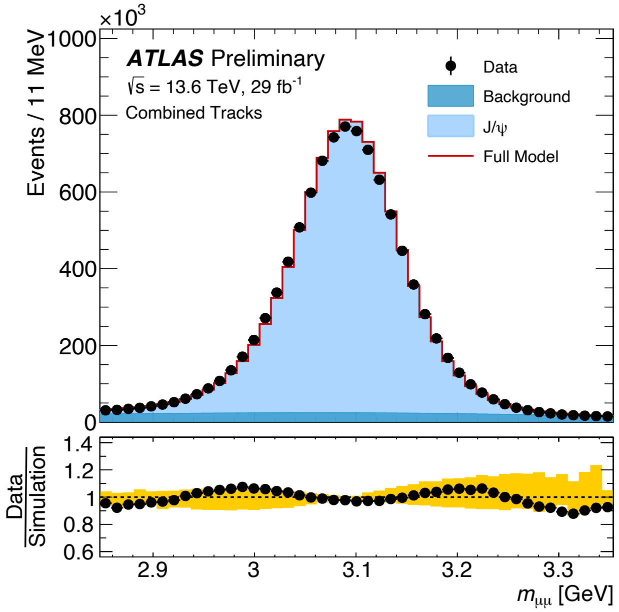

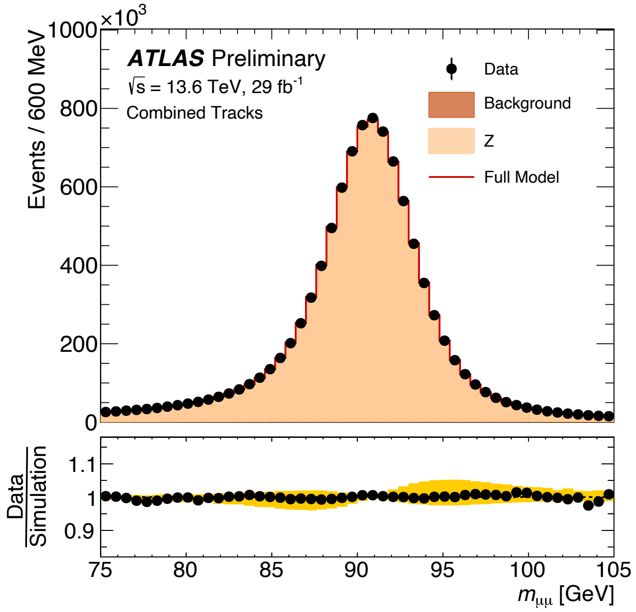

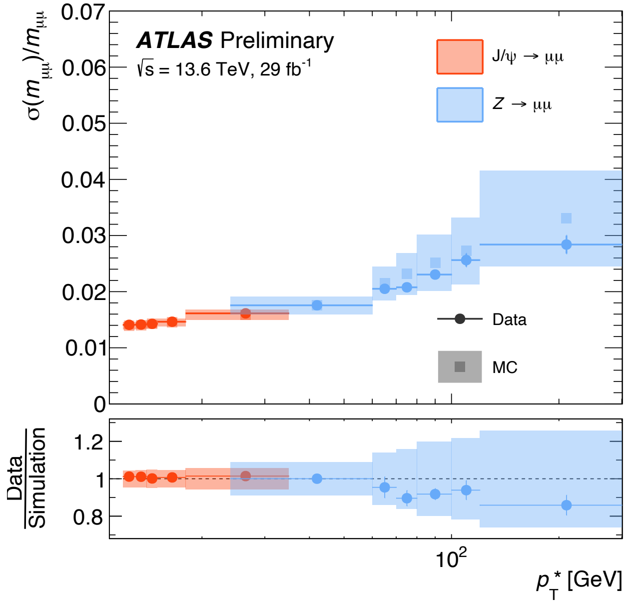

- Good dimuon mass resolution (1.6-2.6%).

Analysis strategy

- Select events with **two opposite-charge high pT muons** + quality requirements
- Improve the invariant mass resolution by including FSR photons(+4%) and dimuon vertex refit(+2%).

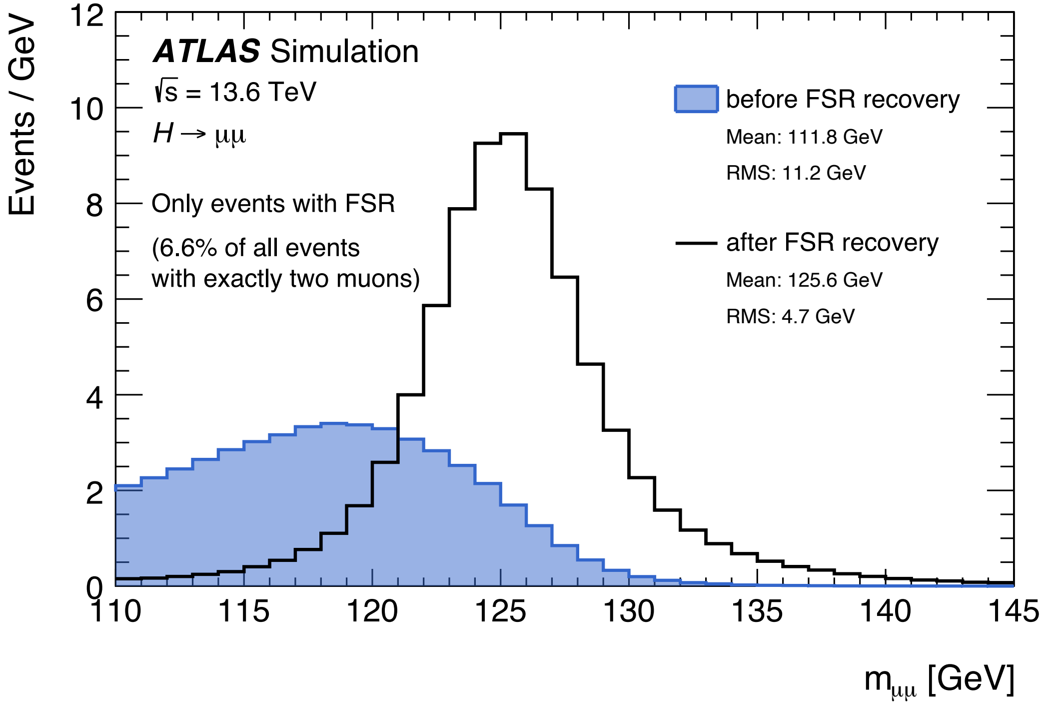

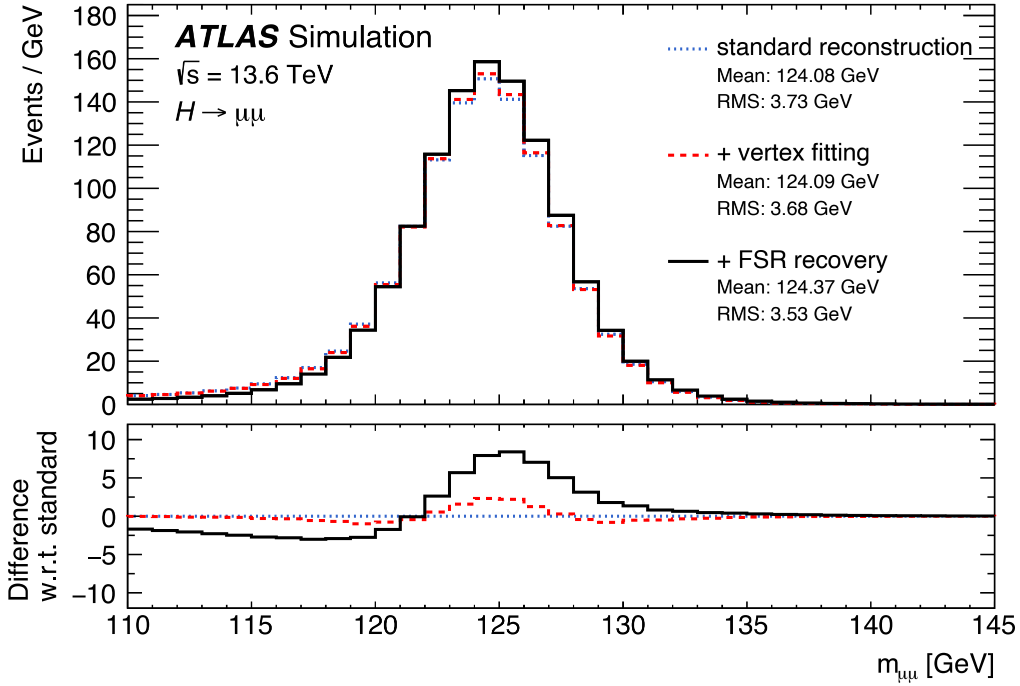

- **Categorize events** to improve the inclusive signal-to-background ratio.
- **Data driven analytic fit**: extract signal from a binned, maximum likelihood S+B fit of the dimuon mass distribution in the 110-160 GeV range.

Categorization workflow

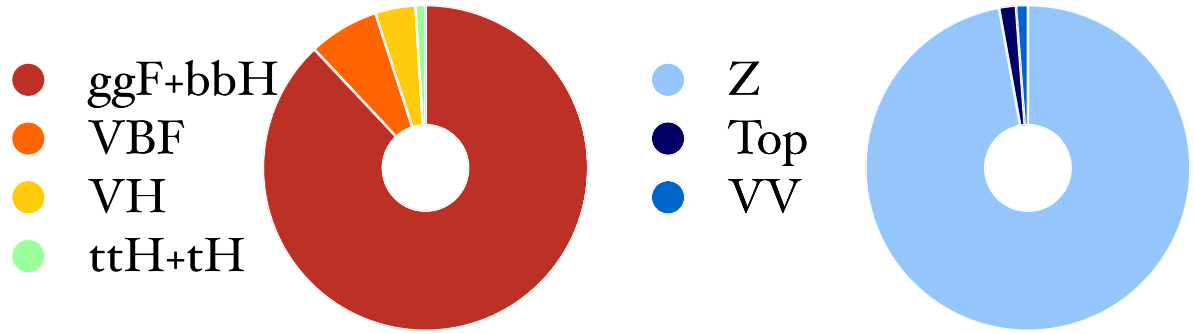

Higgs boson production modes

Backgrounds

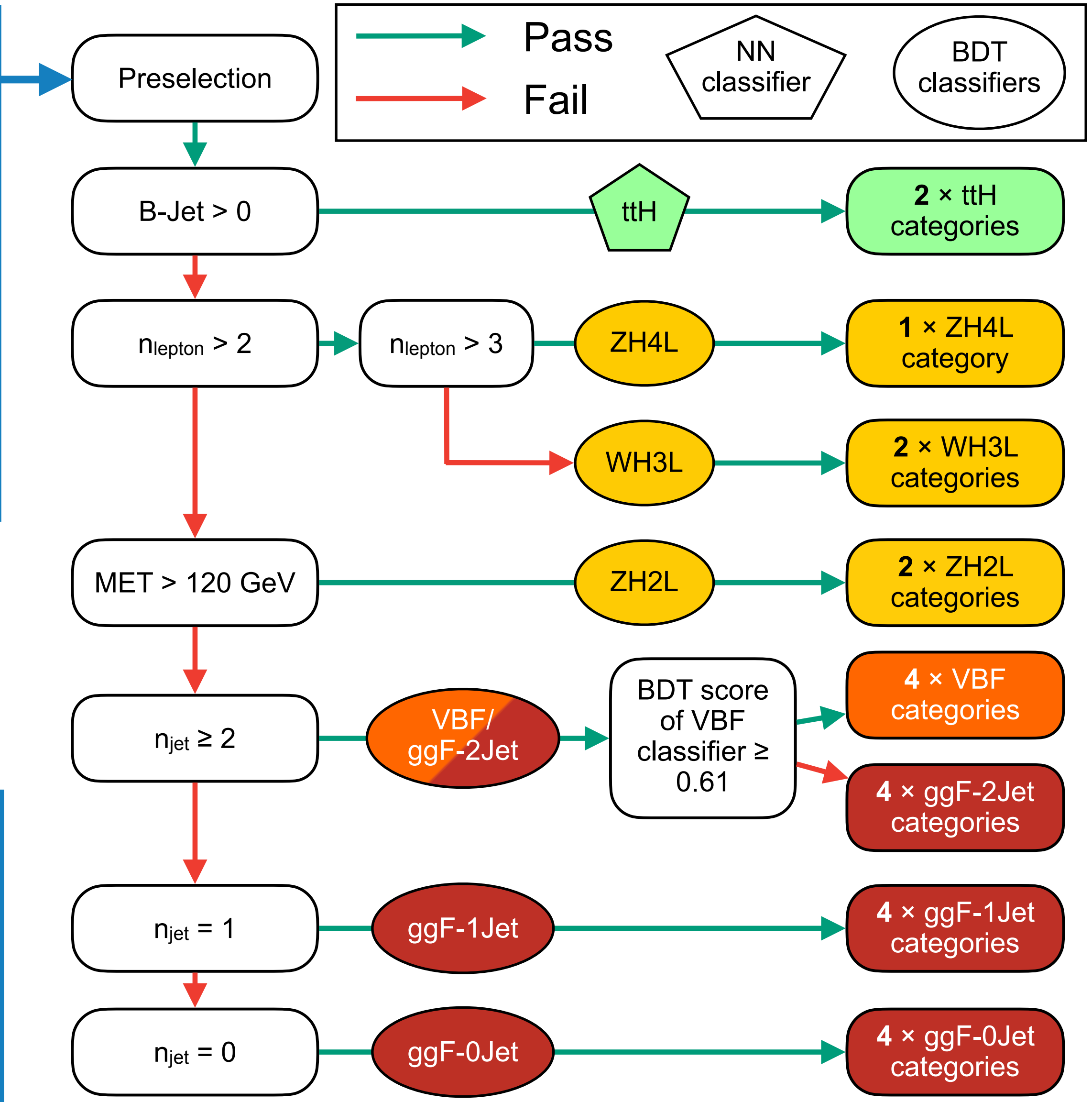

- Sort events into mutually exclusive categories, targeting the various Higgs boson production modes
- Category boundaries optimized for maximize sensitivity

- Preselections:
  - Muons: $|\eta| < 2.5$, Leading (Sub) $p_T > 27$ (15) GeV
  - Jets: $p_T > 25$ GeV and $|\eta| < 2.4$, or $p_T > 30$ GeV and $|\eta| < 4.5$
  - B-tagging efficiency: GN2 WP of 85%

ttH and VH categories

- Tagging the ttH and VH events with the decay products of top/Z/W.
  - **ttH categories**: events with at least one b-tagged jet
    - Used distance correlation neural-network classifier to avoid correlation to dimuon mass
  - **ZH4L category:** events with 4-leps
    - Dilepton pair with mass closest to the Z boson is labeled as the Z-boson candidate

$$\chi^2 = a(\frac{m_{l_1 l_2} - m_H}{\sigma_H})^2 + (\frac{m_{l_3 l_4} - m_Z}{\sigma_Z})^2$$

  - **WH3L category**: events with 3-leps
    - Pairing the leptons

$$\chi^2 = (\frac{m_{\mu_1\mu_2} - m_H}{\sigma_H})^2 + (\frac{m^T_{\mu_3,MET} - m^T_W}{\sigma^T_W})^2$$

  - **ZH2L category**: events with 2-leps and large Missing E_T (>120 GeV)
    - Targeting Z boson's decay to neutrinos

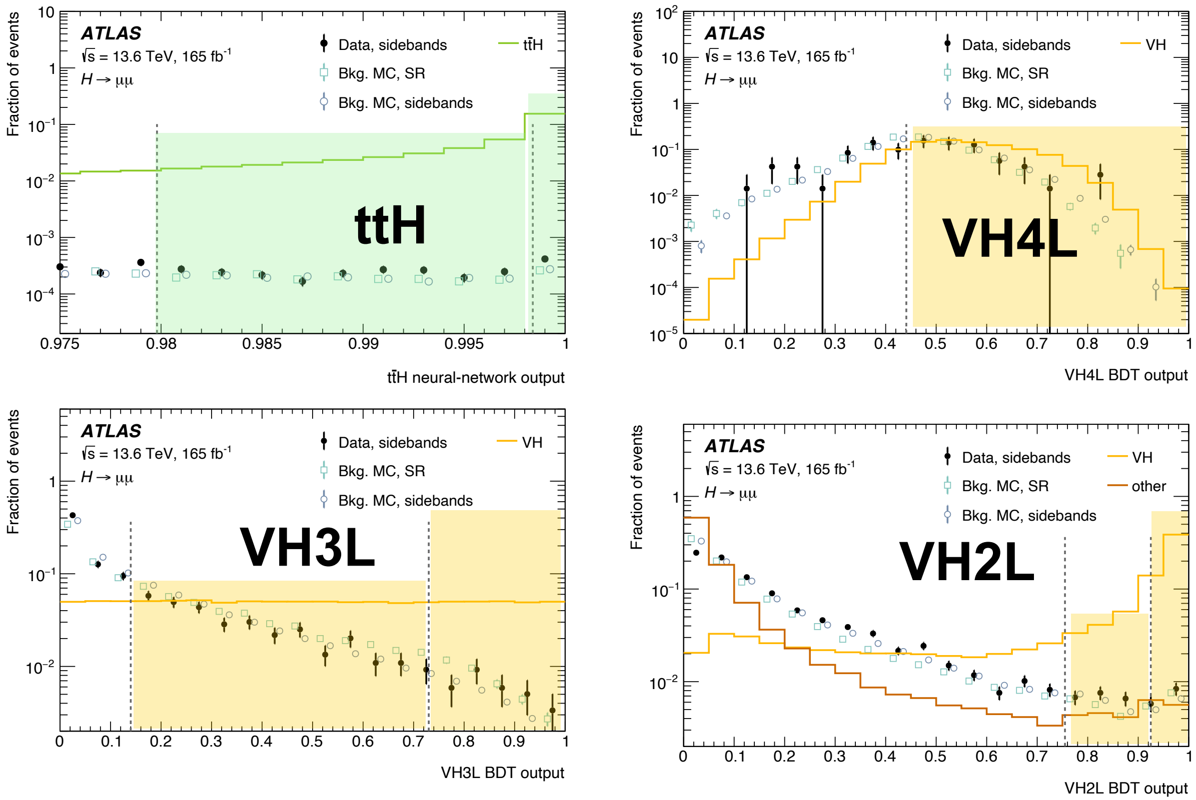

VBF and ggF categories

- Remaining events from the ttH and VH selections.
  → no extra leptons, no b-tagged jet, Missing E_T <120 GeV
  - **VBF categories**: events with at least 2 jets
    - 2-D boundary optimization with ggF 2-jets categories
  - **ggF 2/1/0-jet categories**:
    - Exploit boost of dimuon pT, central η etc.

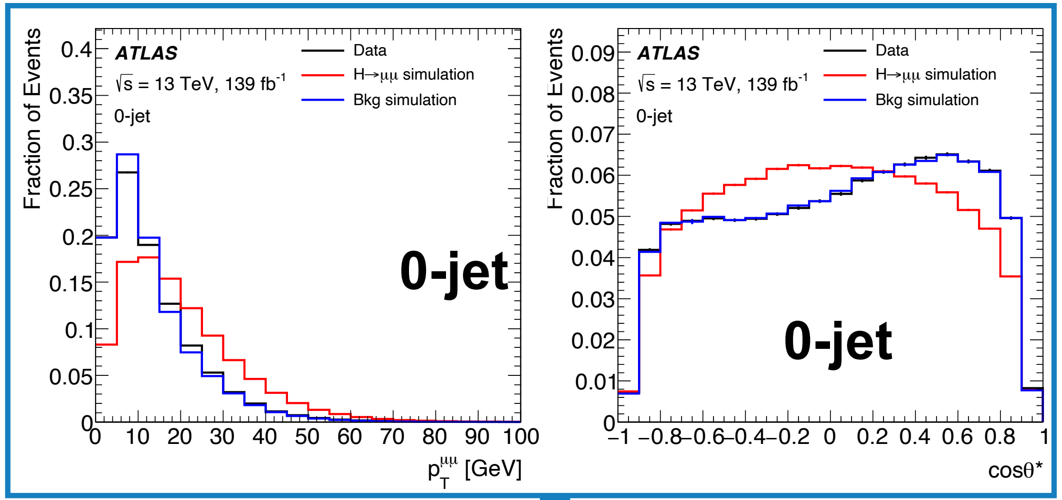

- All the classifiers used multi-fold approach to maximum use of the MC events and to avoid from over training.

Events	25%	25%	25%	25%	Final
1st fold	Training	Training	Validation	Test	Test
2st fold	Test	Training	Training	Validation	Test
3st fold	Validation	Test	Training	Training	Test
4st fold	Training	Validation	Test	Training	Test

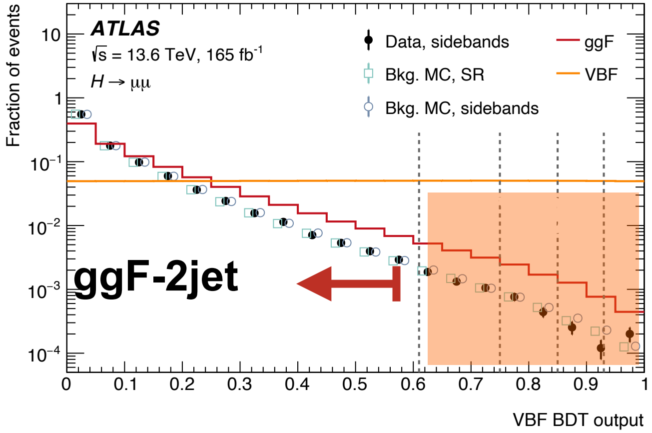

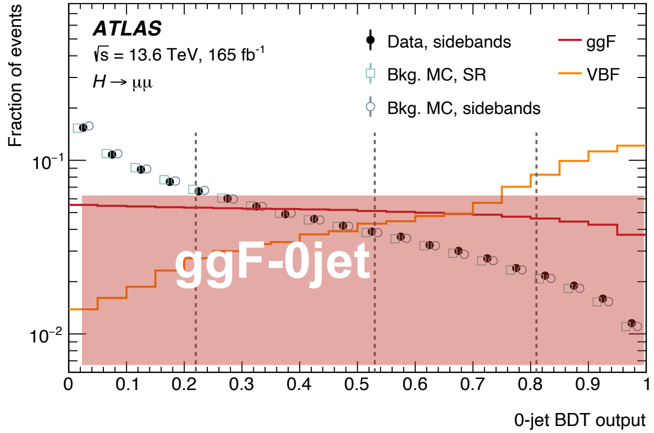

Summary of the categorization

- A total of 23 category and good separation between the different production modes
- Sensitivity expected to driven by ggF and VBF categories
  - DY background dominant in the ggF/VBF categories
- S/B ranging from <**0.1%** (0-jet Very Low) to ~**20%** (VBF High)

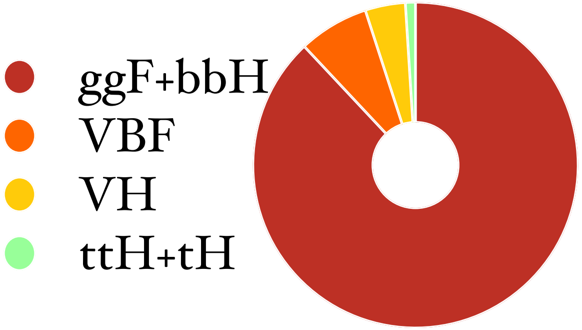

Higgs boson production modes

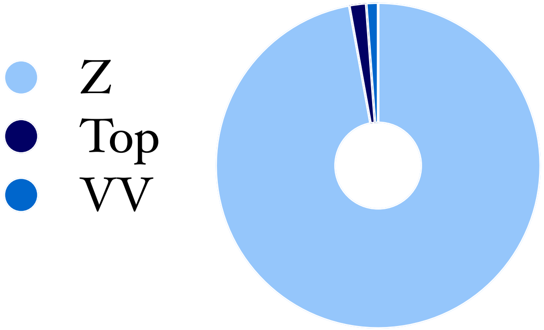

Backgrounds

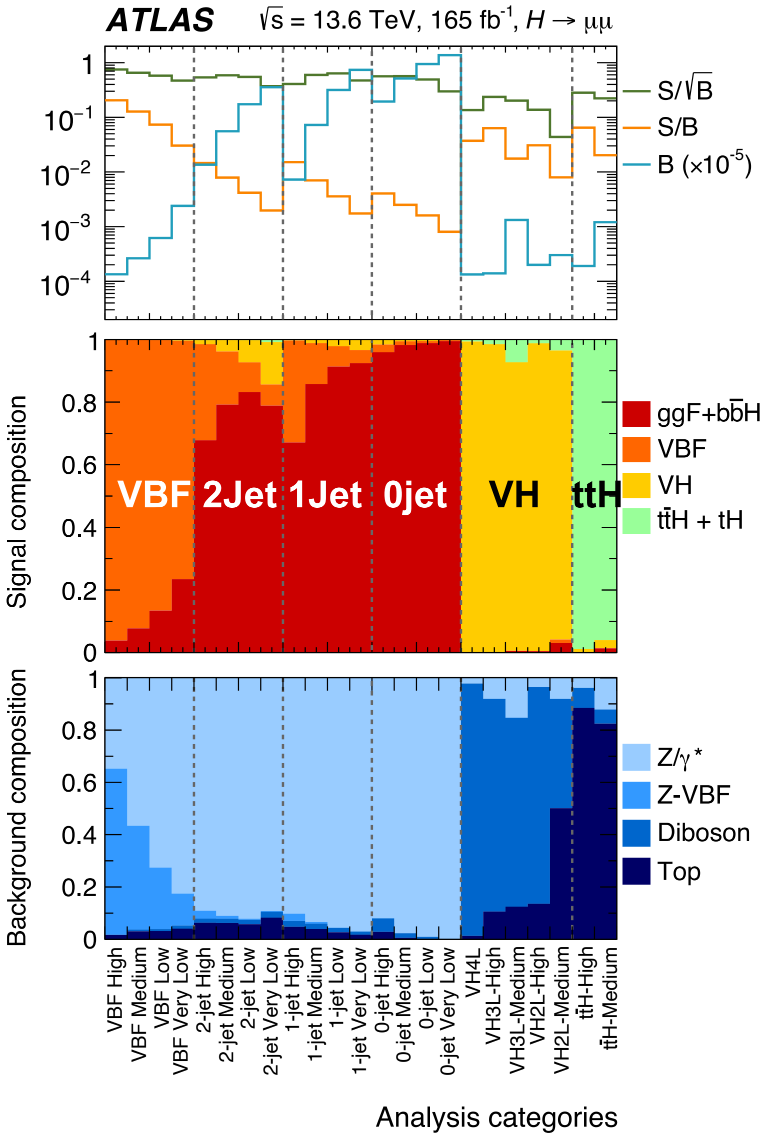

Signal modeling

- SM Higgs boson width only 4 MeV → Signal shape dominated by detector resolution(~3 GeV)

- MC spectra created by summing over all production modes in each category
- Using Double-Sided Crystal Ball (DSCB) as analytic parameterization for the signal by fitting to MC spectra.
  - Crystal Ball width ranges from 2.8 to 3.2 GeV

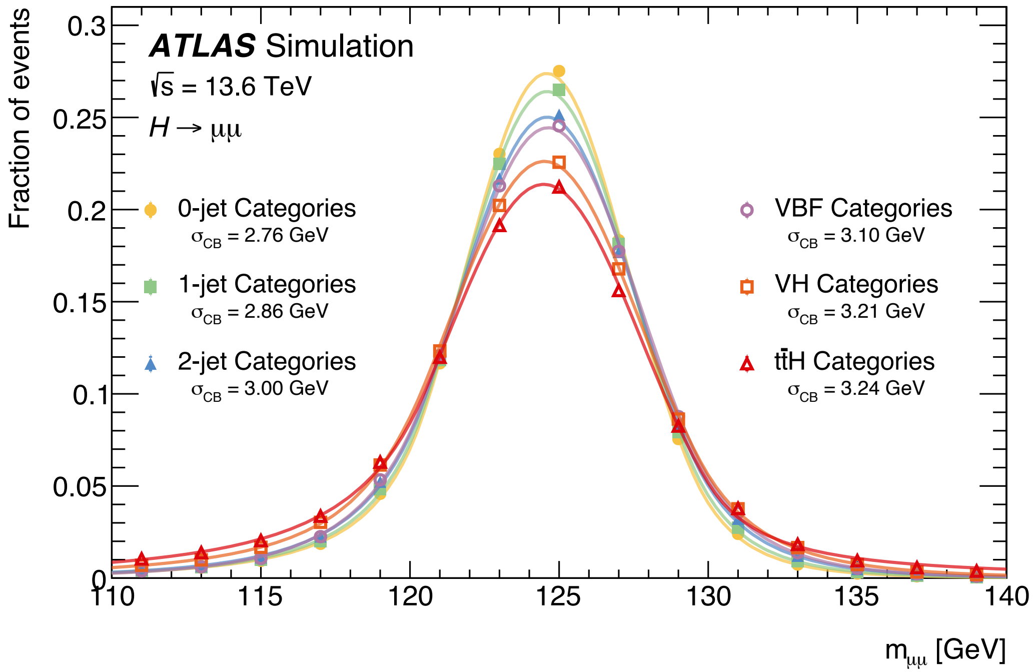

- Systematic uncertainties → **in general negligible compared to data statistics**
  - **Theory**: BR, QCD scale, PDF uncertainties (all modes); Underlying event, parton showering (ggF/VBF)
  - **Experimental**: Higgs mass, muon momentum (and Jet energy) scale and resolution, luminosity, Reconstruction efficiencies (e/μ/b-tag/jet), forward jet mismodeling, pileup modeling.

Background modeling: data-driven sideband fit

- As S/B is generally quite low → Per-mille level precision necessary to avoid biases in extracted signal yields
- Requires a large number of simulated events
  - Used 5 billion (NLO) Drell–Yan fully simulated high-mass ($m_{\mu\mu}$ > 105 GeV) enriched sample

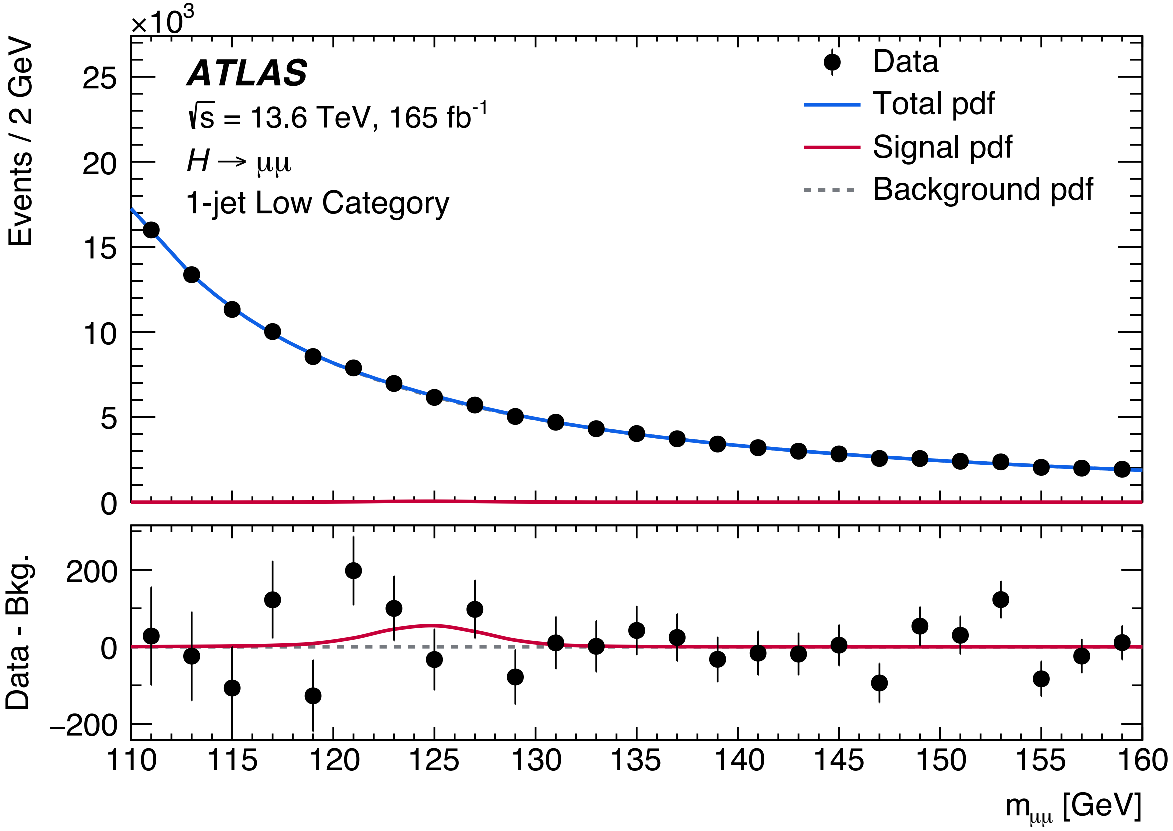

- Dimuon mass spectrum parameterized with "**core×empirical**" background models
  - **Core function**: fully rigid LO Drell-Yan line-shape convoluted with detector resolution
    - Capture the steepness of the DY background
  - **Empirical function**: handle the remaining bias between core function and template

Background modeling: definition of the models

- As S/B is generally quite low → Per-mille level precision necessary to avoid biases in extracted signal yields

$$DY_{LS}(m_{\mu\mu}) = \sum_q \mathcal{L}_{q\bar{q}} \cdot \sigma_{q\bar{q}} \cdot m_{\mu\mu}\ ,\ q = u,\ s,\ d,\ c,\ b$$

- Requires a large number of simulated events
  - Used 5 billion (NLO) Drell–Yan fully simulated high-mass ($m_{\mu\mu}$ > 105 GeV) enriched sample

- Dimuon mass spectrum parameterized with "core×empirical" background models
  - **Core function**: fully rigid LO Drell-Yan line-shape convoluted with detector resolution
    - Capture the steepness of the DY background
  - **Empirical function**: handle the remaining bias between core function and template

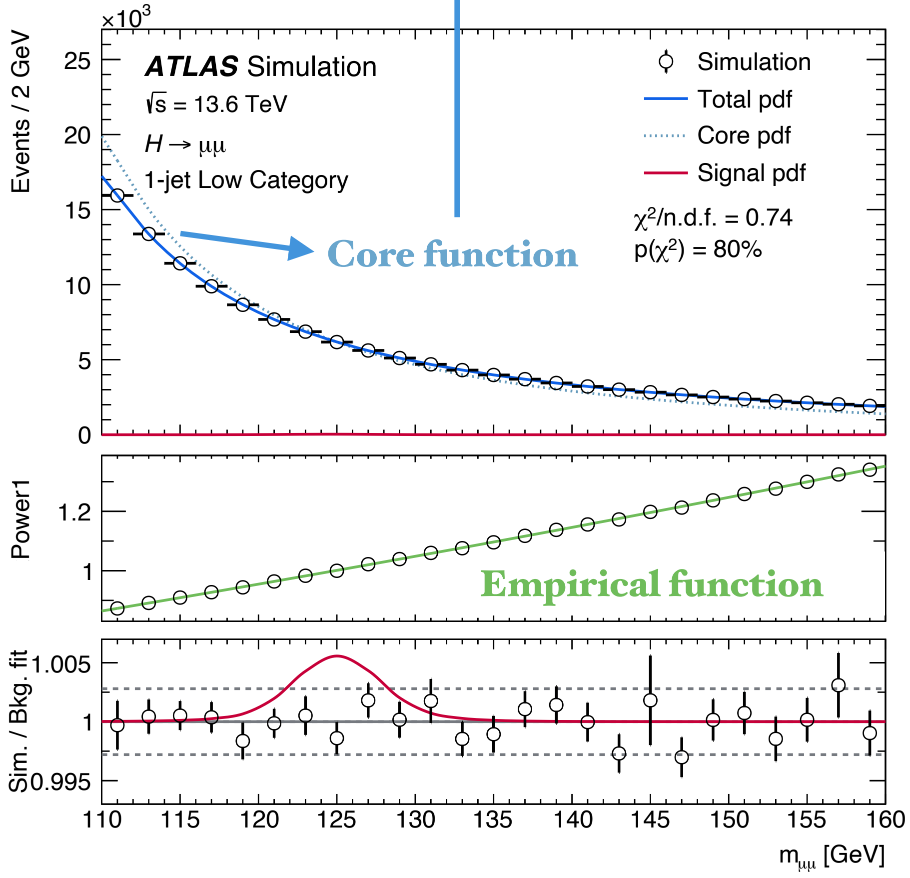

Background modeling: choice of the models

- Empirical function Determine by **spurious signal test**:
  - Fit **S+B model** to a **bkg. only MC template**, maximum value of fitted signal yield in range [120, 130] GeV called "spurious signal" (SS).
  - Require:
    - SS < 20% of the uncertainty from the data statistical fluctuation
    - χ^2 probability of the bkg. only fit > 1%
  - Select the model with the **smallest number of free parameters** then with the **smallest SS** among the functions met the above requirements.
  - SS taken as background model systematic.

- Tested candidates
  - EpolyN $\rightarrow$ $exp(a_0 + a_1 m_{\mu\mu} + \ldots + a_N m_{\mu\mu}^N)$
  - PowerN $\rightarrow$ $m_{\mu\mu}^{(a_0 + a_1 m_{\mu\mu} + \ldots + a_N m_{\mu\mu}^N)}$

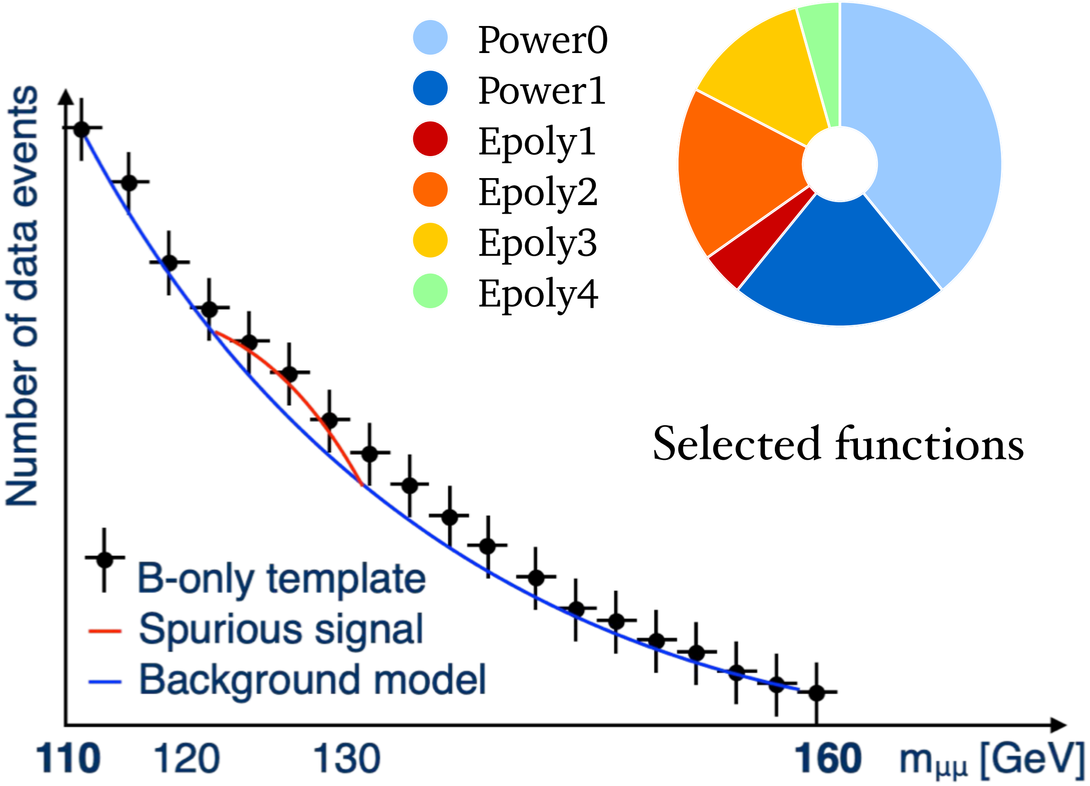

Selected functions

Run3 results

- Best fit value of the signal strength: (m_H = 125.09 GeV)
  - Run3: $\mu(\sigma/\sigma_{SM}) = 1.6 \pm 0.6$
- Significance wrt bkg. Only hypothesis:
  - Observed: **2.8 σ**
  - Expected: **1.8 σ**

Uncertainty source	$\Delta\mu$	
Statistical uncertainty	-0.55	+0.55
Systematic uncertainty	-0.18	+0.24
Spurious signal	-0.14	+0.15
Theory	-0.08	+0.13
Luminosity	-0.04	+0.08
Muon	-0.03	+0.07
Jets, flavor tagging	-0.02	+0.03
Other	-0.04	+0.07
Total	-0.57	+0.60

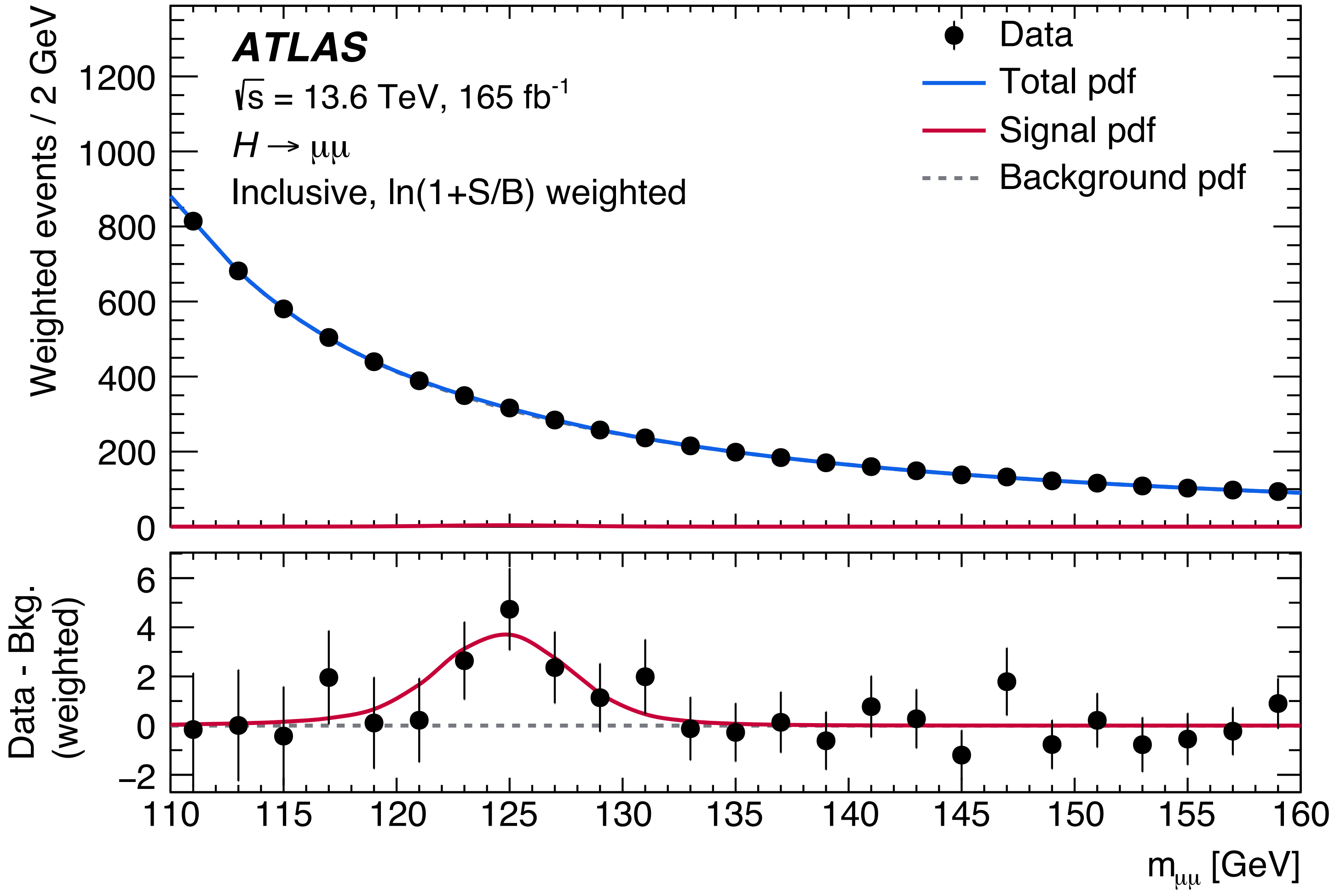

Run3 + Run2 combination

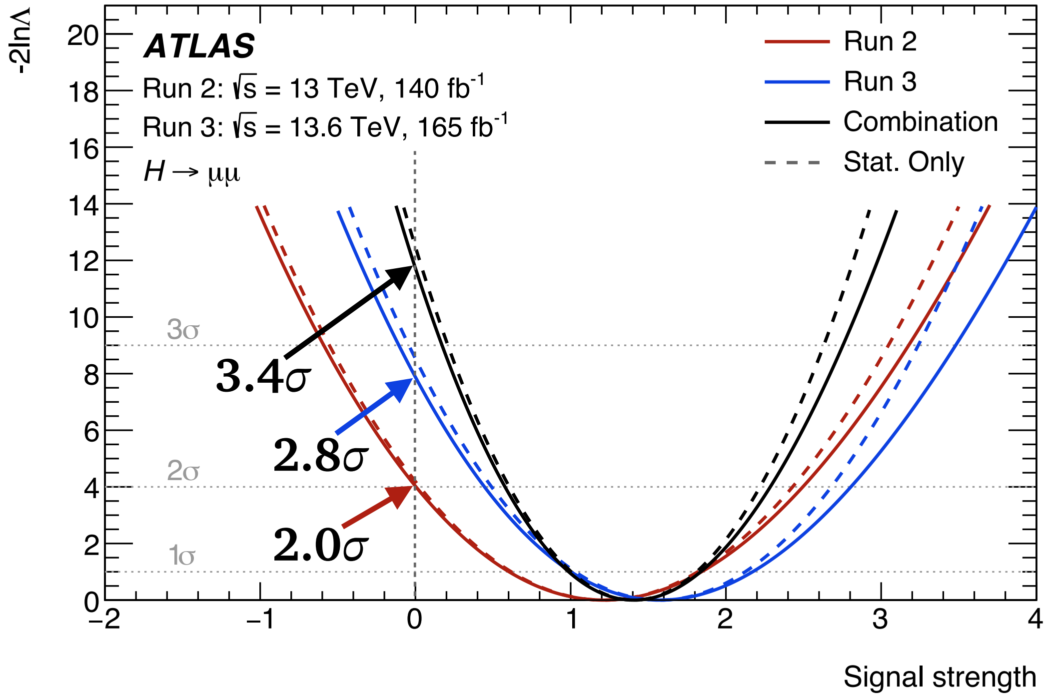

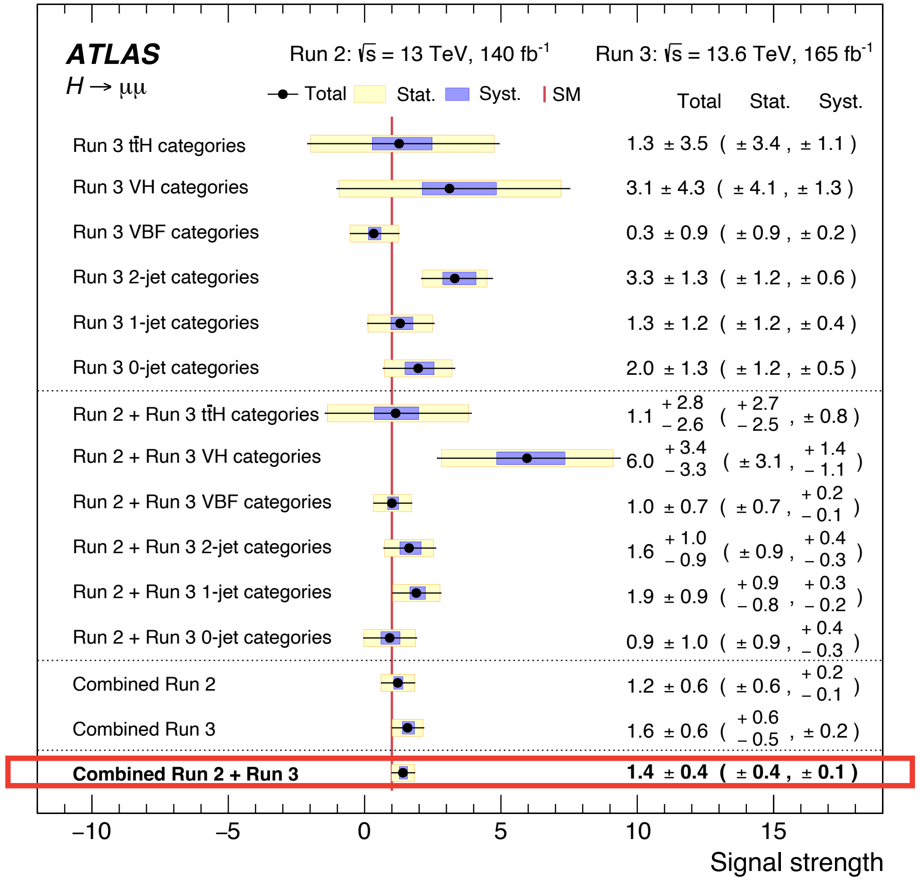

- Significance wrt bkg. Only hypothesis:
  - Expected: **2.5 σ**

    Combination improves Run 2 results **by 50%**
  - Observed: **3.4 σ**

    Clear evidence of $H \rightarrow \mu^+\mu^-$ decay!

The measurement of signal strengths across Run 2 and Run 3 are compatible, corresponding to a p-value of 0.68.

Run3 + Run2 results

- Best fit value of the signal strength: (m_H = 125.09 GeV)
  - Run3 + Run2: $\mu(\sigma/\sigma_{SM}) = 1.4 \pm 0.4$

Uncertainty source	$\Delta\mu$	
Statistical uncertainty	-0.40	+0.41
Systematic uncertainty	-0.12	+0.15
Spurious signal	-0.09	+0.09
Theory	-0.07	+0.10
Luminosity	-0.02	+0.04
Muon	-0.02	+0.04
Jets, flavor tagging	-0.01	+0.01
Other	-0.02	+0.03
Total	-0.42	+0.43

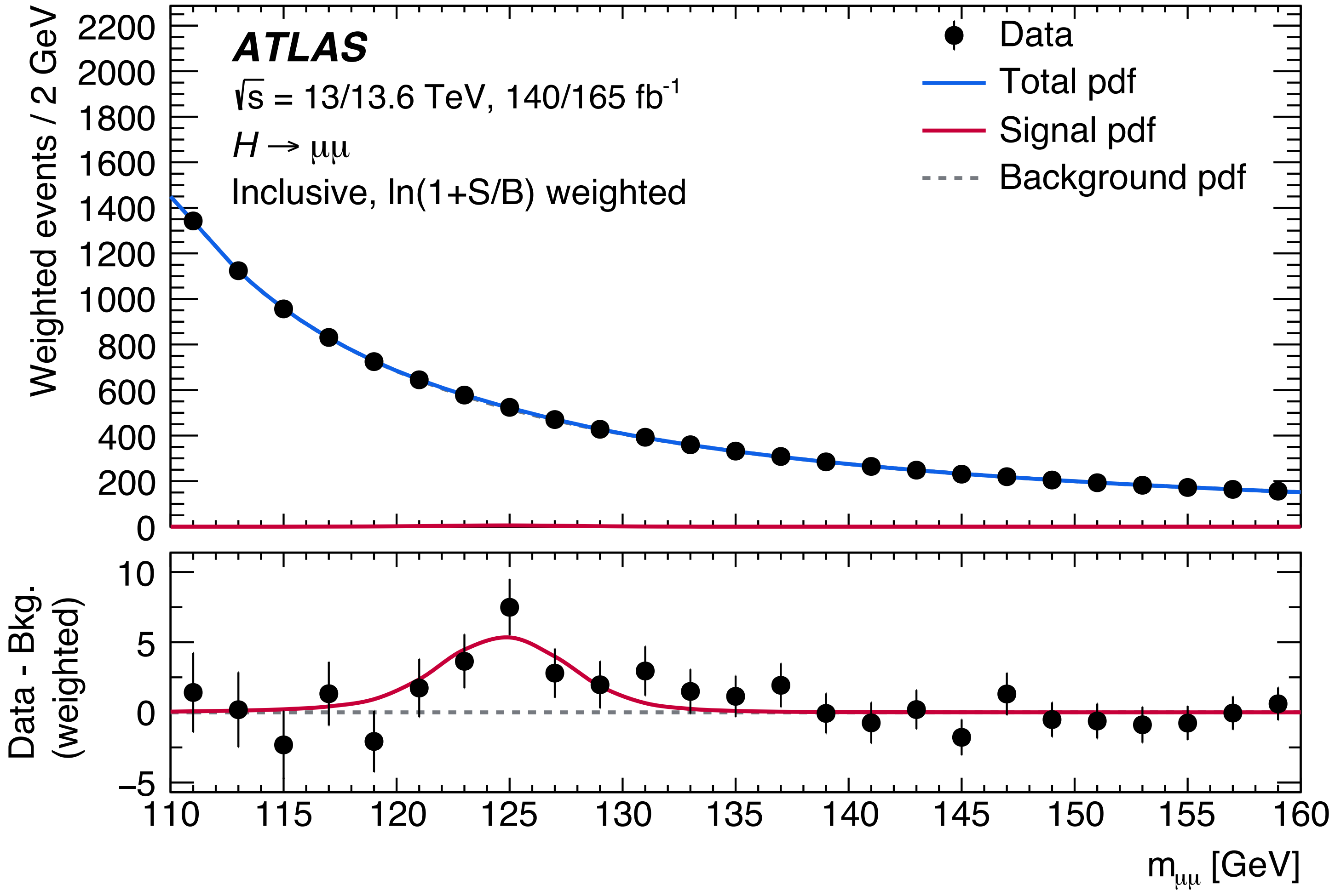

Run3 + Run2 results

- Best fit value of the signal strength:
  (m_H = 125.09 GeV)
  - Run3 + Run2: $\mu(\sigma/\sigma_{SM}) = 1.4 \pm 0.4$

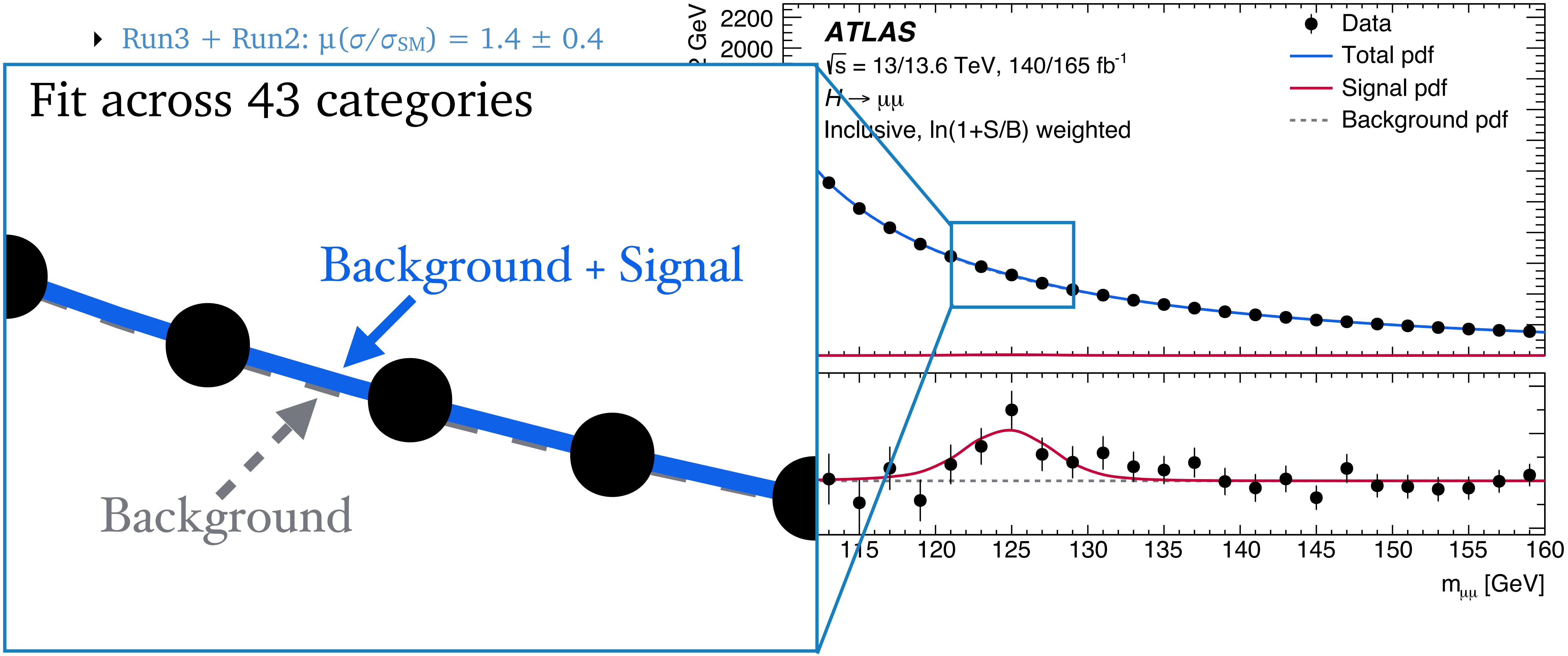

Summary

- First ATLAS evidence of H→μμ declared with Run 3+2 data:
  - Signal strength of **1.4 ± 0.4 = 1.4 ± 0.4 (stat.) ± 0.1 (syst.)**, **evidence at 3.4σ!**
  - Still limited by statistical uncertainty
  - [Link to paper](), [CERN Courier]()
    Accepted by PRL (editor's suggestions)

ATL-PHYS-PUB-2025-014

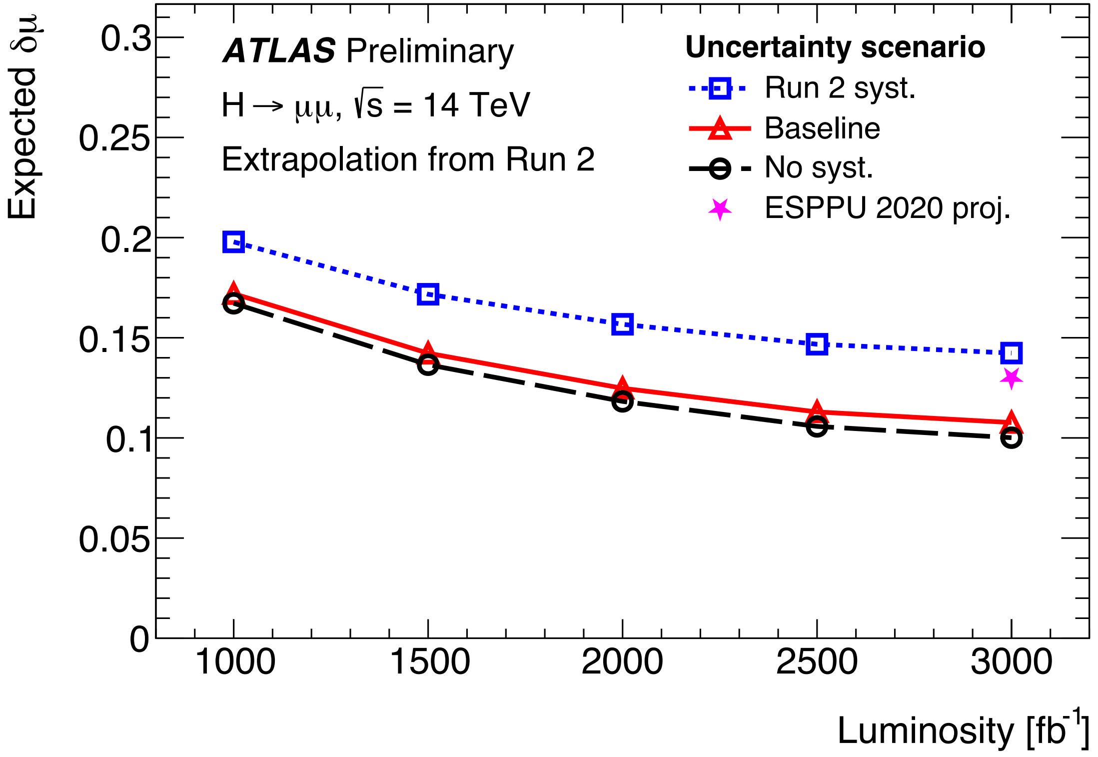

- Outlook:
  - Increased integrated luminosity
    in Run 3. Expect ~300 fb^{-1} @13.6 TeV
  - And not in very far future: High Luminosity LHC

Thanks for your attention!

Back up materials

Event selection

- Select events with **two opposite-charge high pT muons** + quality requirements

	Selection
Common preselection	Primary vertex Two opposite-charge muons Muons: $\lvert\eta\rvert < 2.5$, $p_{\mathrm{T}}^{\mathrm{lead}} > 27\,\mathrm{GeV}$, $p_{\mathrm{T}}^{\mathrm{sublead}} > 15\,\mathrm{GeV}$
Fit region	$m_{\mu\mu} = 110 - 160\ \mathrm{GeV}$
Jets	$p_{\mathrm{T}} > 25\,\mathrm{GeV}$ and $\lvert\eta\rvert < 2.4$ or with $p_{\mathrm{T}} > 30\,\mathrm{GeV}$ and $2.4 < \lvert\eta\rvert < 4.5$
b-tagged jets	$p_{\mathrm{T}} > 25\,\mathrm{GeV}$ and $\lvert\eta\rvert < 2.4$ or with $p_{\mathrm{T}} > 30\,\mathrm{GeV}$ and $2.4 < \lvert\eta\rvert < 2.5$ Tagging efficiency working point of 85%
$t\bar{t}H$ categories	At least one b-jet
VH 4-lepton category	Exactly two additional e or μ with $p_{\mathrm{T}} > 8\,\mathrm{GeV}, 5\,\mathrm{GeV}\ (\mu)\ /\ 7\,\mathrm{GeV}\ (e)$, no b-jets
VH 3-lepton categories	Exactly one additional e or μ with $p_{\mathrm{T}} > 15\,\mathrm{GeV}$, no b-jets
VH 2-lepton categories	No additional lepton, no b-jets, $E_{\mathrm{T}}^{\mathrm{miss}} > 120\ \mathrm{GeV}$
VBF and ggF categories	No additional lepton, no b-jets, $E_{\mathrm{T}}^{\mathrm{miss}} < 120\ \mathrm{GeV}$

FSR recovery

- Muons from the $H\to\mu\mu$ decay can lose their energy by Final State Radiation(FSR).
  - Large E_T, Small ΔR from μ
- Improve the invariant mass resolution by including FSR photons. (~5%)
- Currently applied to categories only contain two muons (ggF, VBF, $Z_{\nu\nu}H_{\mu\mu}$).
  - Far candidates are excluded with $\Delta R < 0.2$ cut to suppress photons from $H\to Z(\mu\mu)\gamma$ decay
  - Only near candidates are used, fake FSR suppressed via E_T cut: $E_T > 25\text{ GeV} \cdot \Delta R(\mu,\gamma) + 3\text{ GeV}$

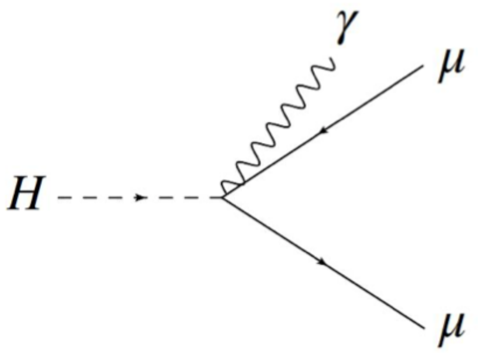

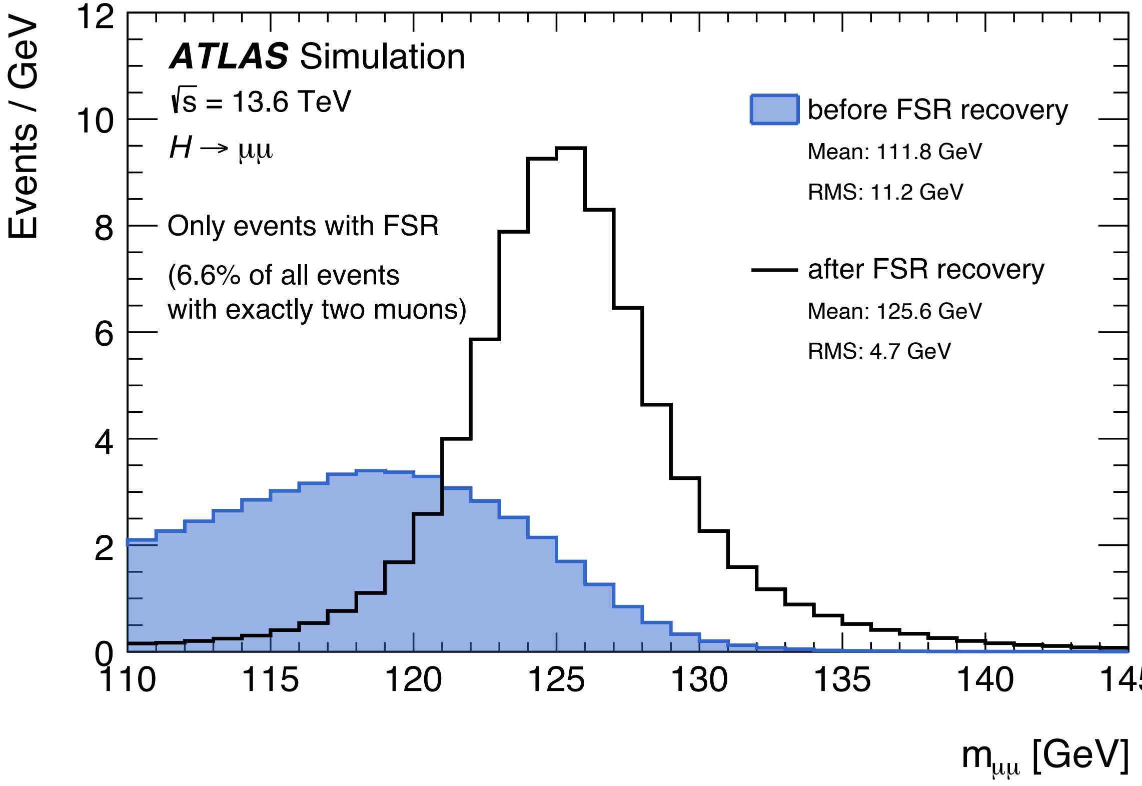

- The event reconstruction is improved by fitting the decay vertex of di-muon system.
  - A more precise value for d_0 → a better estimate of $m_{\mu\mu}$.
  - A narrower di-muon peaks: Z($\mu\mu$), H($\mu\mu$)
    - Invariant mass resolution improved ~2%.

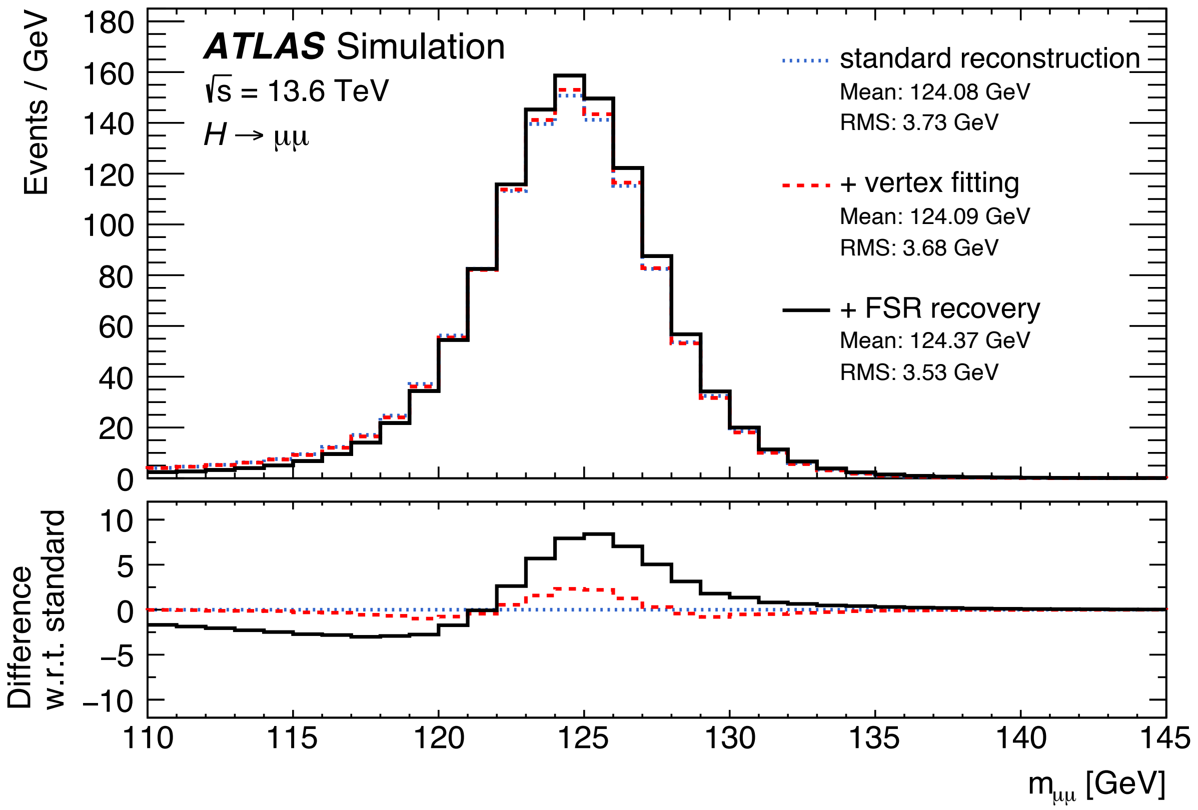

Training variables for categorization

- ttH

Variable	Description
$p_{\mathrm{T}}^{\mu_1}$	Transverse momentum of the leading muon
$p_{\mathrm{T}}^{\mu_2}$	Transverse momentum of the sub-leading muon
η^{μ_1}	Pseudorapidity of the leading muon
η^{μ_2}	Pseudorapidity of the sub-leading muon
ϕ^{μ_1}	Azimuthal angle of the leading muon
ϕ^{μ_2}	Azimuthal angle of the sub-leading muon
N_{μ}	Number of muons
$\cos\theta^*$	μ^- decay angle in the Collins–Soper frame
$p_{\mathrm{T}}^{j_1}$	Transverse momentum of the leading jet
$p_{\mathrm{T}}^{j_2}$	Transverse momentum of the sub-leading jet
η^{j_1}	Pseudorapidity of the leading jet
η^{j_2}	Pseudorapidity of the sub-leading jet
$N_{\mathrm{Track}}^{j_1}$	Number of tracks in the leading jet with $p_{\mathrm{T}} > 0.5$ GeV
$N_{\mathrm{Track}}^{j_2}$	Number of tracks in the sub-leading jet with $p_{\mathrm{T}} > 0.5$ GeV
m^{jj}	Invariant mass of the dijet system
H_{T}^{j}	Scalar sum of jet transverse momentum
$N_{j-\mathrm{central}}$	Number of central ($\lvert\eta\rvert < 2.5$) jets
$N_{b-\mathrm{jet}}$	Number of b-jets with 85% working point
$E_{\mathrm{T}}^{\mathrm{miss}}$	Missing transverse energy
N_e	Number of electrons
$p_{\mathrm{T}}^{\ell_3}$	Transverse momentum of the third lepton
$p_{\mathrm{T}}^{\ell_4}$	Transverse momentum of the fourth lepton
m^{sub}	Mass of leading non-Higgs-boson-candidate muon and opposite-sign Higgs-boson-candidate muon
$m^{\ell_3\ell_4}$	Mass of third and fourth leptons
$\Delta\phi(\ell_3,\ell_4)$	Azimuthal angle between the third and fourth leptons
$\Delta\eta(\ell\ell,\ell_3)$	Pseudorapidity separation between the dimuon system and third lepton
$m_{\mathrm{T}}^{\mathrm{t\text{-}Lep}}$	Transverse mass of leptonic top-quark decay
$m^{\mathrm{t\text{-}Had}}$	Mass of hadronic top-quark decay
$m_{\mathrm{T}}^{W\text{-}\mathrm{Lep}}$	Transverse mass of leptonic W-boson decay
$m^{W\text{-}\mathrm{Had}}$	Mass of hadronic W-boson decay

- ZH4L

Variable	Description
$p_{\mathrm{T}}^{\mathrm{pair}_1}$	Transverse momentum of the first pair of leptons
$p_{\mathrm{T}}^{\mathrm{pair}_2}$	Transverse momentum of the second pair of leptons
$p_{\mathrm{T}}^{\mathrm{pair}_1\ \ell_1}$	Transverse momenta of the leading lepton of the first pair
$\Delta R(\mathrm{pair}_1,\mathrm{pair}_2)$	ΔR between the first and second pair
$\Delta R(\ell_1,\ell_2)$	ΔR between the leading leptons of each pair
$\alpha(\mathrm{pair}_1,\mathrm{pair}_2)$	Opening angle between the lepton pairs
$\log_{10}(-u)$, $\log_{10}(-t)$	Mandelstam $u-$ and t-variables
H_{T}^{ℓ}	Scalar sum of transverse momentum of the four leptons
$p_{\mathrm{T}}{}^{\ell_i}$ $(i=2,3,4)$	p_{T} of the second, third and fourth lepton
$\lvert\eta_{\mathrm{forward}}\rvert$	Pseudorapidity of most forward lepton pair
$\alpha_{CMF}(\ell_1^{\mathrm{pair}_1},\ell_2^{\mathrm{pair}_1})$	Opening angle between leptons of Z-like pair (or pair_1) in center-of-mass frame
$\theta_{CMF}(\mathrm{pair}_2)$	Polar angle of H-boson candidate pair (or pair_2) in center-of-mass frame

- WH3L

Variable	Description
$p_{\mathrm{T}}^{\ell_W}$	Transverse momentum of the W-boson lepton
$E_{\mathrm{T}}^{\mathrm{miss}}$	Missing transverse energy
m_{T}^{W}	Transverse mass of the W boson
N_j	Number of jets
N_{μ}	Number of muons
$\Delta R(\mu,\mu)$	ΔR between the Higgs-boson candidate muons
$\cos\theta^*$	μ^- decay angle in the Collins–Soper frame
$m^{3\ell}$	Invariant mass of the three leptons
$p_{\mathrm{T}}^{j_1}$	Transverse momenta of the leading jet
$\Delta\phi(\ell\ell,\ell_W)$	Azimuthal angle between the muon pair and the W-boson lepton
$\Delta\eta(\ell\ell,\ell_W)$	Pseudorapidity separation between muon pair and W-boson lepton
$\Delta\phi(\ell\ell,E_{\mathrm{T}}^{\mathrm{miss}})$	Azimuthal angle between the muon pair and the missing transverse momentum

Training variables for categorization

- VBF and ggF2/1/0- Jets

Variable	Description	$n_j = 0$	$n_j = 1$	$n_j \geq 2$ and VBF
$p_{\mathrm{T}}^{\mu\mu}$	Transverse momentum of muon pair	x	x	x
$Y^{\mu\mu}$	Rapidity of muon pair	x	x	x
$\cos\theta^*$	μ^- decay angle in the Collins–Soper frame	x	x	x
$p_{\mathrm{T}}^{j_1}$	Transverse momentum of leading jet		x	x
η^{j_1}	Pseudorapidity of leading jet		x	x
$\Delta\phi(\mu\mu, j_1)$	Azimuthal angle between the muon pair and the leading jet		x	x
$N_{\mathrm{Track}}^{j_1}$	Number of tracks in leading jet with $p_{\mathrm{T}} > 0.5$ GeV		x	x
$p_{\mathrm{T}}^{j_2}$	Transverse momentum of sub-leading jet			x
η^{j_2}	Pseudorapidity of sub-leading jet			x
$\Delta\phi(\mu\mu, j_2)$	Azimuthal angle between the muon pair and the sub-leading jet			x
$N_{\mathrm{Track}}^{j_2}$	Number of tracks in sub-leading jet with $p_{\mathrm{T}} > 0.5$ GeV			x
p_{T}^{jj}	Transverse momentum of dijet system			x
Y^{jj}	Rapidity of dijet system			x
$\Delta\phi(\mu\mu, jj)$	Azimuthal angle between the muon pair and the dijet system			x
m^{jj}	Invariant mass of dijet system			x
$E_{\mathrm{T}}^{\mathrm{miss}}$	Missing transverse energy			x
H_{T}^{j}	Scalar sum of jet transverse momentum			x

- $Z(\nu\nu)H(\mu\mu)$

Variable	Description
$p_{\mathrm{T}}^{\mu_1}$	Transverse momentum of leading muon
$p_{\mathrm{T}}^{\mu_2}$	Transverse momentum of sub-leading muon
$E_{\mathrm{T}}^{\mathrm{miss}}$	Missing transverse energy
N_j	Number of jets
$\Delta R(\mu,\mu)$	ΔR between the Higgs-boson candidate muons
$\Delta\phi(\ell\ell, E_{\mathrm{T}}^{\mathrm{miss}})$	Azimuthal angle between the muon pair and the missing transverse momentum
$V_{\mathrm{T}}/H_{\mathrm{T}}$	Ratio of vectorial V_T and scalar H_T sum of reconstructed objects in event
$\cos\theta^*$	μ^- decay angle in the Collins–Soper frame
$\sigma(E_{\mathrm{T}}^{\mathrm{miss}})$	Missing transverse energy significance

Categorization summary

- A total of 23 category

Category	$ggF + b\bar{b}H$	VBF	WH	ZH	$t\bar{t}H + tH$
$t\bar{t}H$-High	0.1%	0.0%	0.5%	0.5%	98.9%
$t\bar{t}H$-Medium	1.4%	0.1%	1.2%	1.3%	96.0%
VH4L	0.0%	0.0%	0.0%	99.3%	0.7%
VH3L-High	0.1%	0.0%	95.1%	3.3%	1.5%
VH3L-Medium	0.5%	0.2%	83.7%	8.3%	7.3%
VH2L-High	0.4%	0.1%	26.1%	72.0%	1.3%
VH2L-Medium	3.1%	1.1%	29.7%	62.5%	3.5%
VBF High	3.9%	96.1%	0.0%	0.0%	0.0%
VBF Medium	7.7%	92.2%	0.0%	0.0%	0.0%
VBF Low	13.4%	86.4%	0.0%	0.1%	0.1%
VBF Very Low	23.4%	76.2%	0.1%	0.1%	0.2%
2-jet High	67.8%	30.7%	0.7%	0.6%	0.2%
2-jet Medium	79.2%	16.9%	2.2%	1.5%	0.2%
2-jet Low	83.2%	9.4%	4.4%	2.7%	0.3%
2-jet Very Low	78.9%	6.7%	8.4%	5.2%	0.8%
1-jet High	67.1%	32.5%	0.2%	0.2%	0.0%
1-jet Medium	85.8%	13.0%	0.7%	0.5%	0.0%
1-jet Low	91.3%	6.5%	1.4%	0.8%	0.0%
1-jet Very Low	92.4%	4.2%	2.2%	1.1%	0.0%
0-jet High	95.9%	2.5%	0.7%	0.9%	0.0%
0-jet Medium	98.3%	1.1%	0.3%	0.3%	0.0%
0-jet Low	98.8%	0.7%	0.2%	0.3%	0.0%
0-jet Very Low	99.5%	0.3%	0.1%	0.1%	0.0%

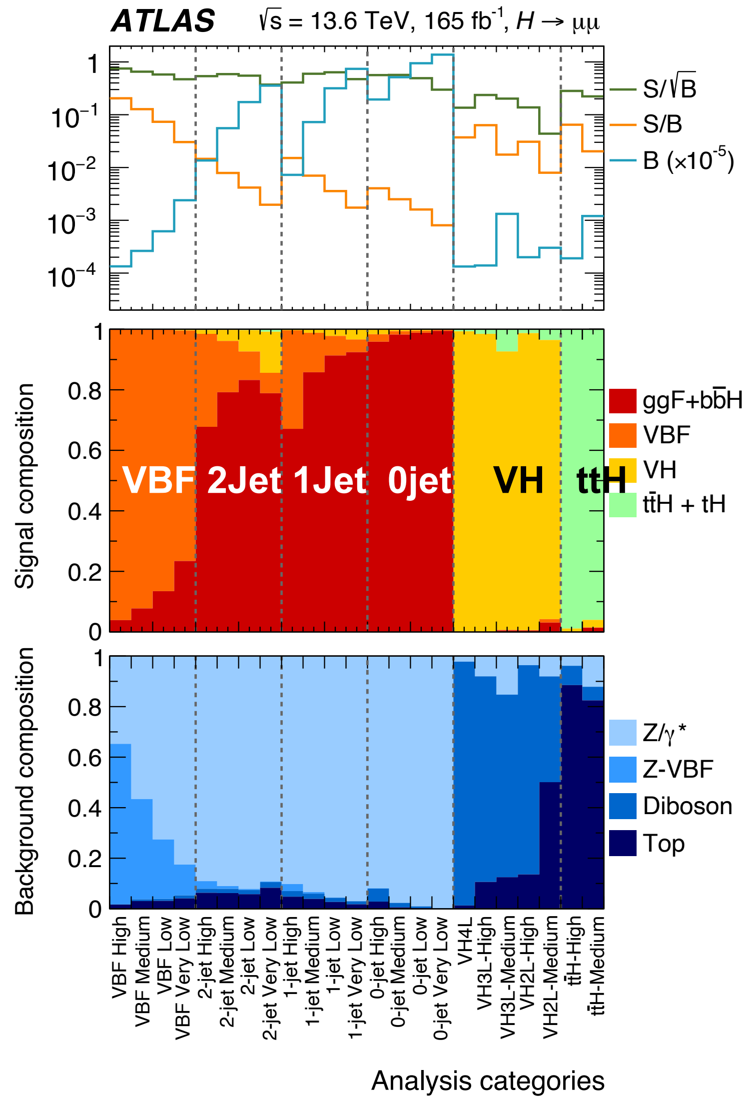

Background models

- Dimuon mass spectrum parameterized with "core×empirical" background models
  - **Core function**: fully rigid LO Drell-Yan line-shape convoluted with detector resolution
    - Capture the steepness of the DY background
    - Updated by including ccbar and bbbar contributions in this round.

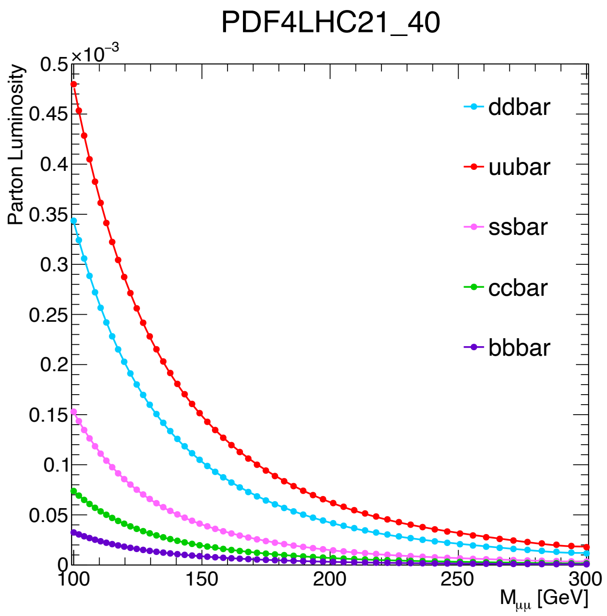

$$DY_{LS}(m_{\mu\mu}) = \sum_{q} \mathcal{L}_{q\bar{q}} \cdot \sigma_{q\bar{q}} \cdot m_{\mu\mu}\ ,\ q = u,\ s,\ d,\ c,\ b$$

- Empirical functions (A total of 23 category)

Category	Empirical Function	max(SS/δS) [%]	max(SS/S_{SM}) [%]
$t\bar{t}H$-High	Power0	31.2	120
$t\bar{t}H$-Medium	Epoly2	13.7	80
VH4L	Power0	-2.01	-30.7
VH3L-High	Epoly2	24.7	156
VH3L-Medium	Epoly4	-25.7	203
VH2L-High	Epoly2	26.8	255
VH2L-Medium	Power0	28	685
VBF High	Power0	16.2	28.8
VBF Medium	Power0	-15.3	-30.4
VBF Low	Epoly1	12.1	-23
VBF Very Low	Power0	21.6	51.4
2-jet High	Epoly2	-27.3	-65.8
2-jet Medium	Power1	-13.6	-24.4
2-jet Low	Power0	29.2	49.7
2-jet Very Low	Power1	38.4	120
1-jet High	Power0	29.8	97
1-jet Medium	Epoly3	-31.6	-72.6
1-jet Low	Power1	16.9	27.2
1-jet Very Low	Power1	32.5	95.4
0-jet High	Power0	43.5	86.2
0-jet Medium	Epoly3	-33.7	-86.1
0-jet Low	Power1	13.5	34.8
0-jet Very Low	Epoly3	-6.89	-37.8

Fit overview

- **VBF-High/Medium/Low/VeryLow**

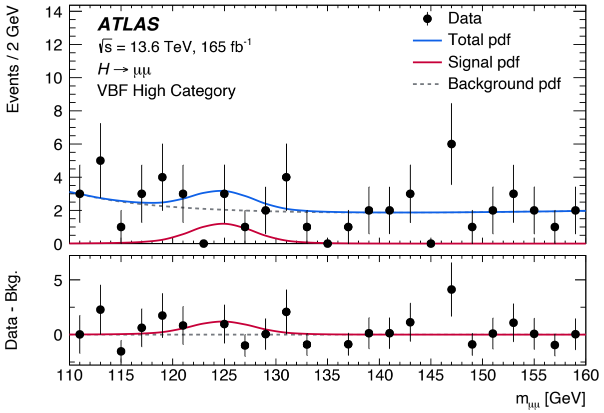

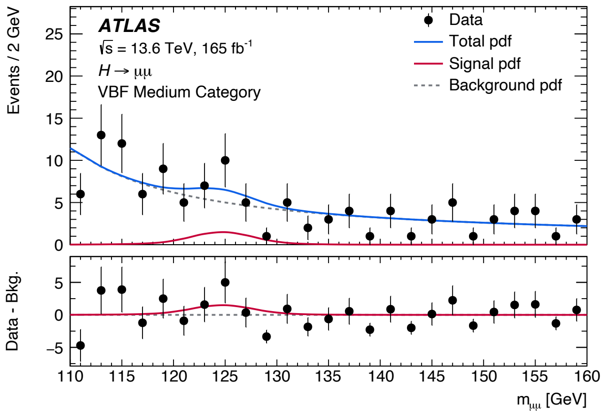

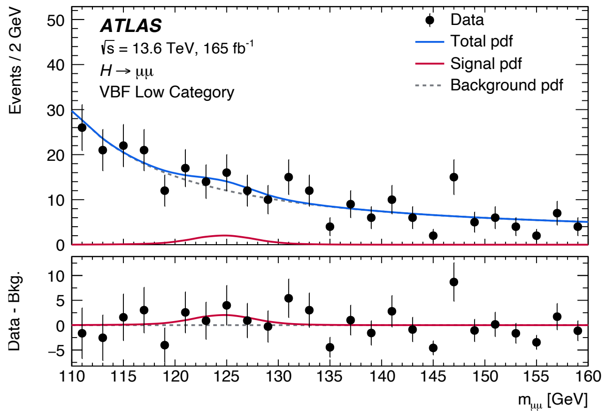

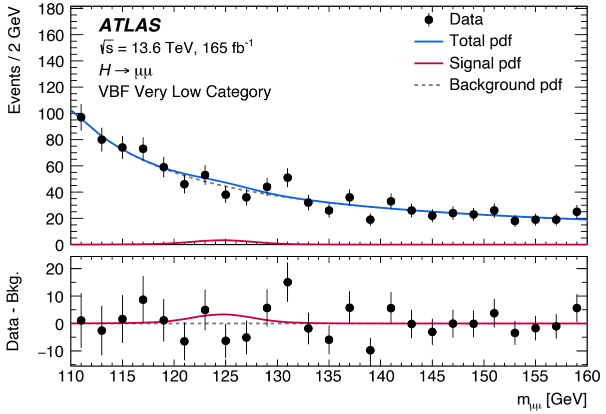

- **Higgs-2Jet-High/Medium/Low/VeryLow**

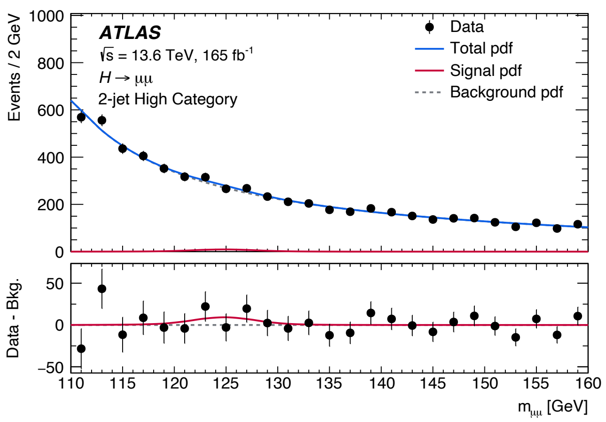

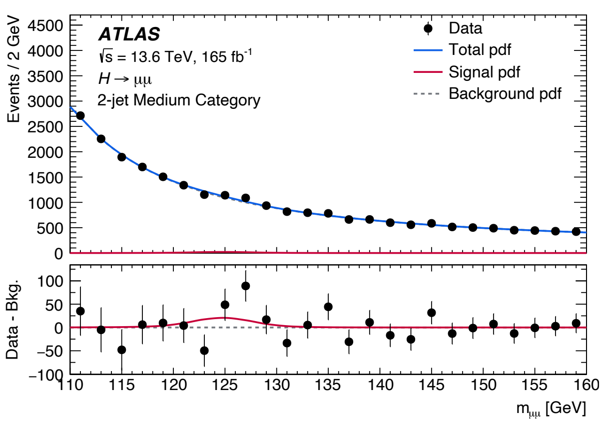

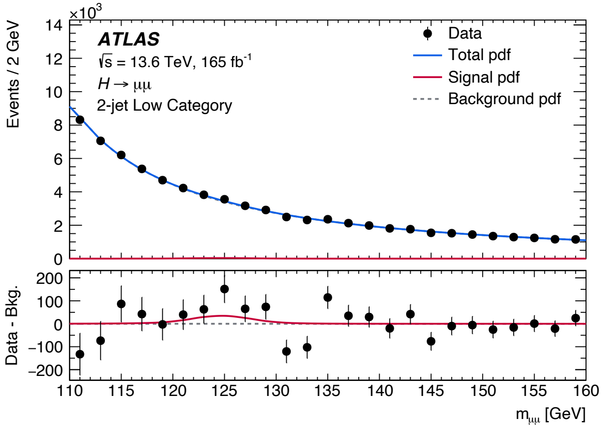

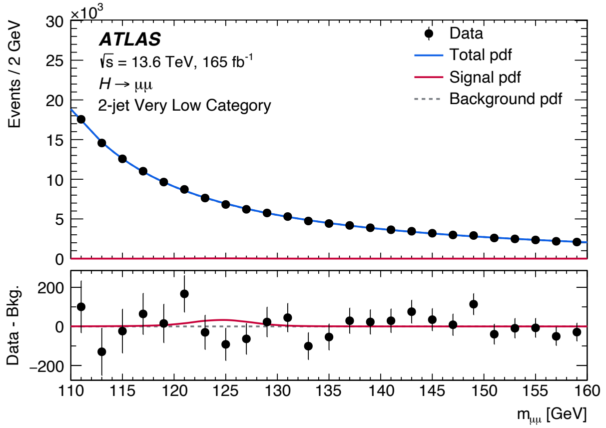

Fit overview

- **Higgs-1Jet-High/Medium/Low/VeryLow**

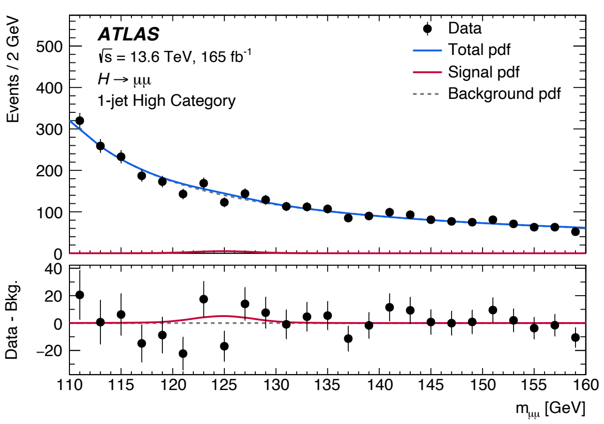

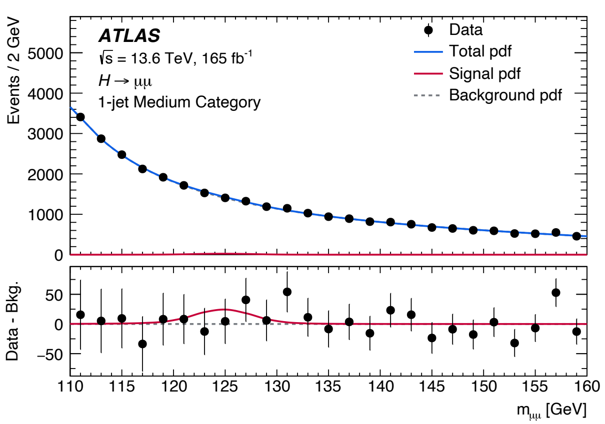

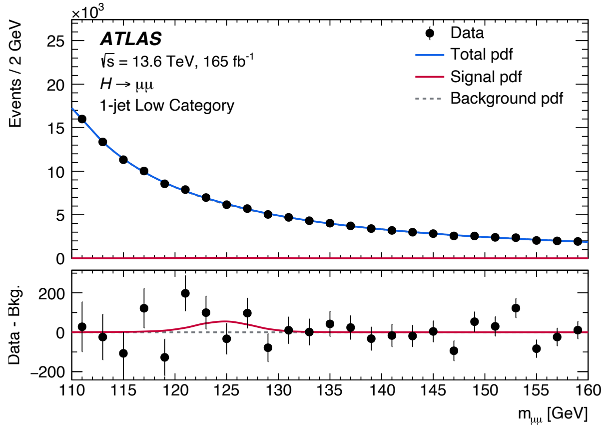

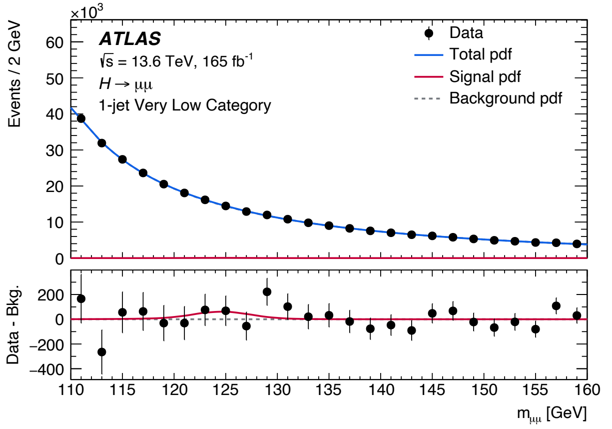

- **Higgs-0Jet-High/Medium/Low/VeryLow**

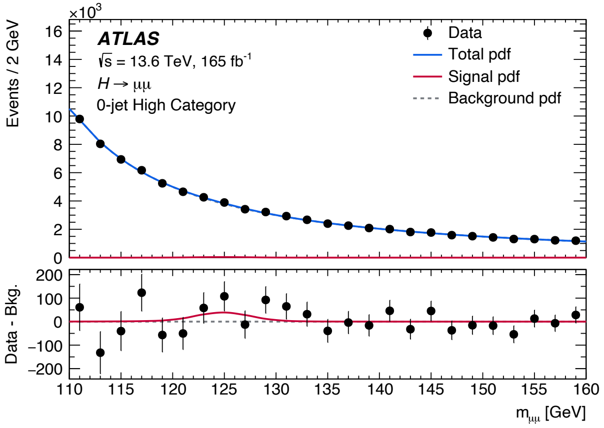

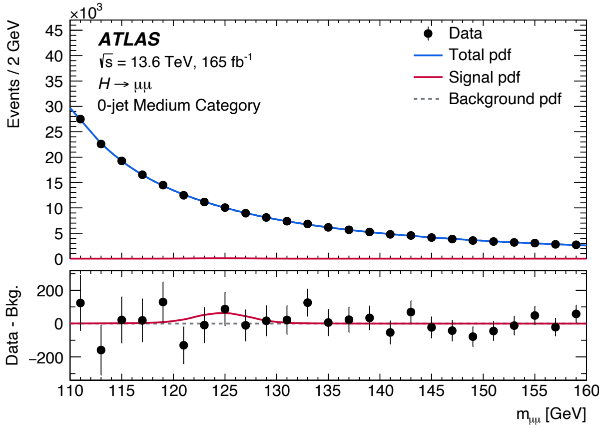

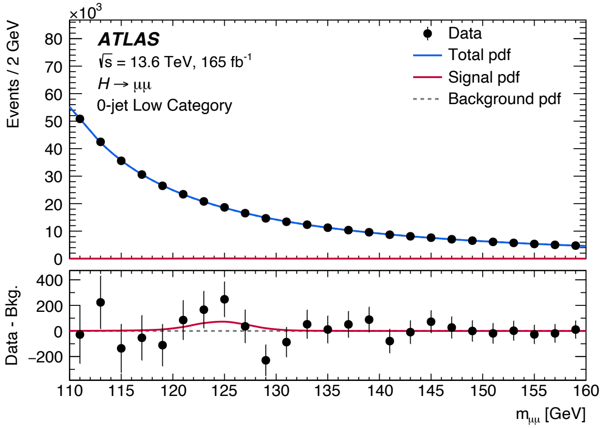

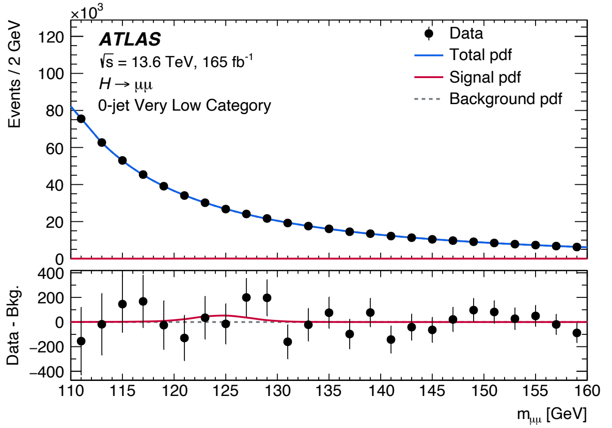

Fit overview

- **VH3L-High/Medium, VH4L**

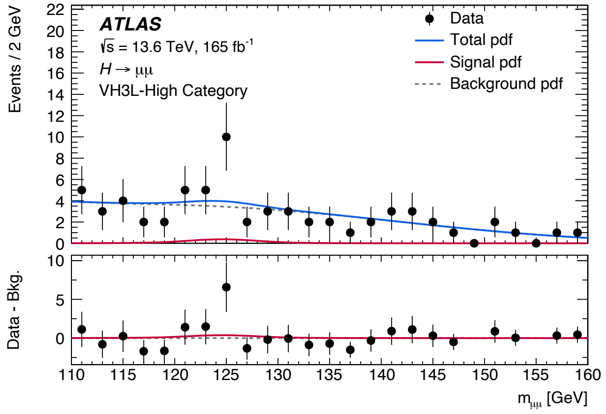

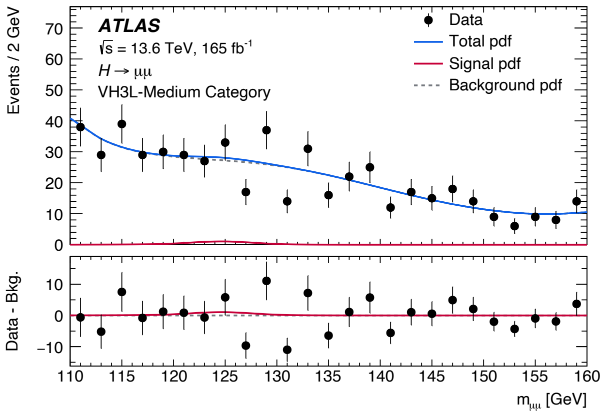

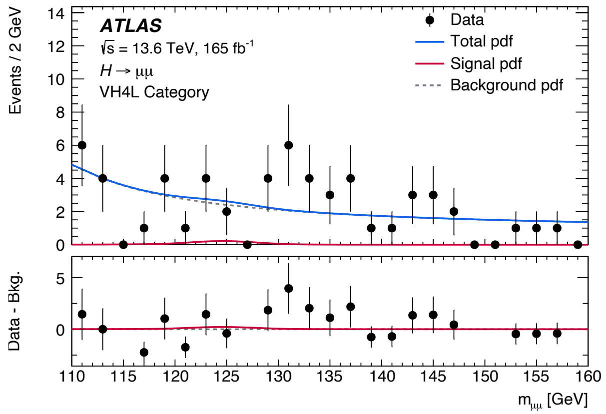

- **ttH-High/Medium, VH2L-High/Medium**

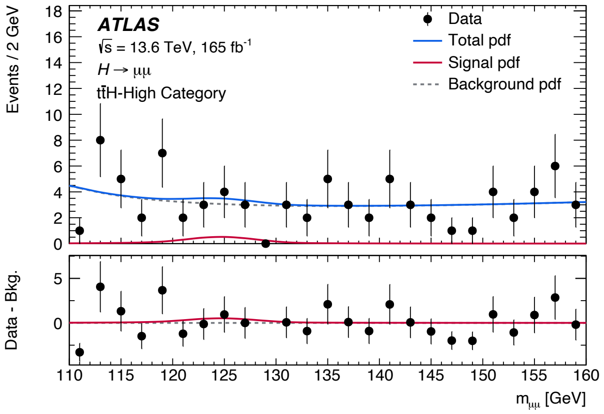

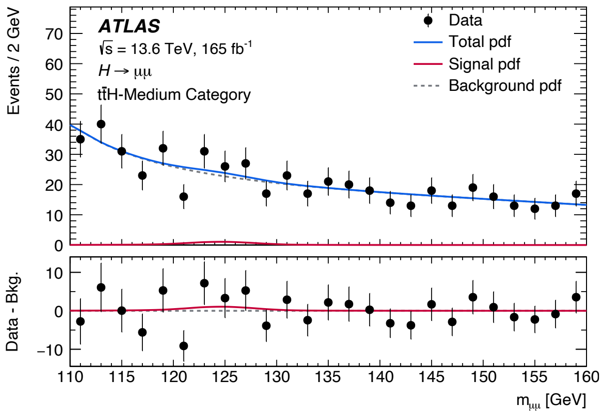

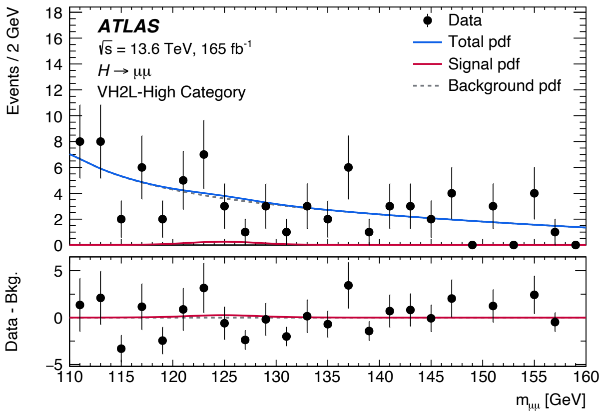

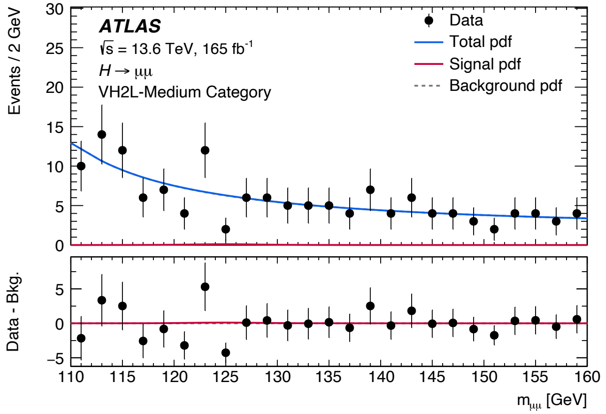

Fit overview

- Profiled likelihood scan

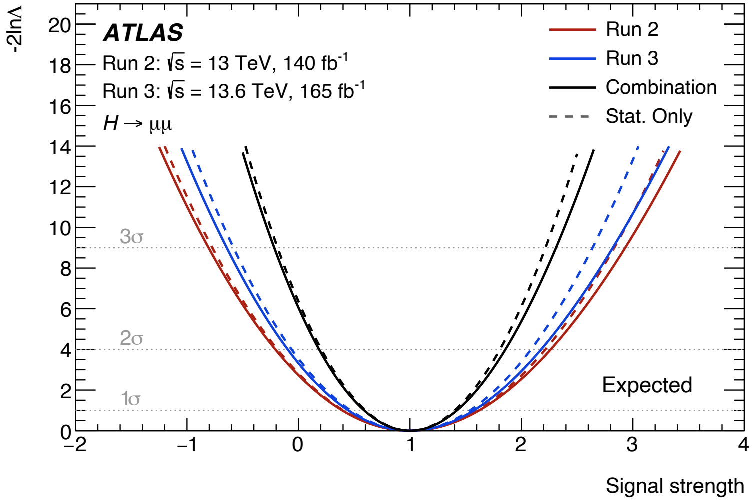

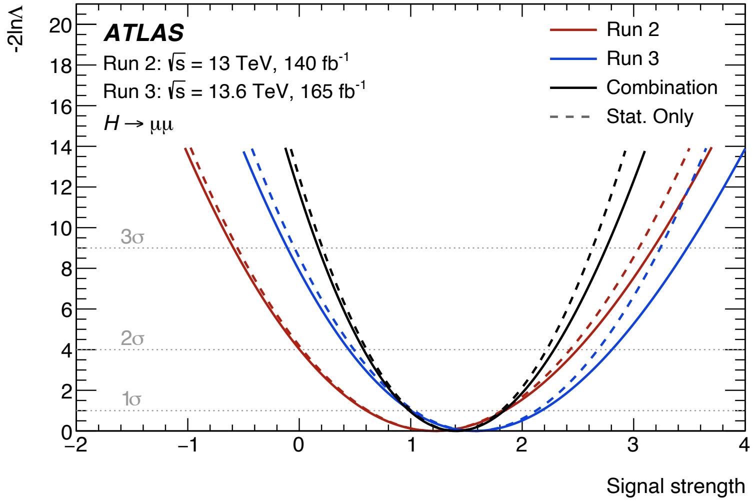

- Fitted yields (observed)

Category	Data	S	B	$S/\sqrt{B}$	S/B [%]
$t\bar{t}H$-High	12	1.9 ± 0.7	15.5 ± 2.3	0.49	12.5
$t\bar{t}H$-Medium	117	3.9 ± 1.4	115 ± 7	0.36	3.4
VH4L	11	0.78 ± 0.29	12.2 ± 1.8	0.22	6.4
VH3L-High	25	1.4 ± 0.5	17.4 ± 2.9	0.33	8.0
VH3L-Medium	143	3.7 ± 1.4	136 ± 10	0.31	2.7
VH2L-High	19	1.0 ± 0.4	18.3 ± 2.9	0.23	5.3
VH2L-Medium	30	0.38 ± 0.14	31.7 ± 3.1	0.07	1.2
VBF High	9	4.3 ± 1.6	10.5 ± 1.8	1.34	41.2
VBF Medium	28	5.3 ± 2.0	25.8 ± 2.7	1.04	20.5
VBF Low	69	7.2 ± 2.7	62 ± 4	0.91	11.6
VBF Very Low	217	11 ± 4	225 ± 8	0.76	5.1
2-jet High	1 399	31 ± 12	$1\,367 \pm 25$	0.84	2.3
2-jet Medium	5 657	69 ± 26	$5\,560 \pm 50$	0.92	1.2
2-jet Low	17 684	110 ± 40	$17\,300 \pm 70$	0.87	0.7
2-jet Very Low	35 147	110 ± 40	$35\,160 \pm 140$	0.59	0.3
1-jet High	708	17 ± 6	710 ± 16	0.65	2.4
1-jet Medium	7 166	80 ± 30	$7\,140 \pm 70$	0.95	1.1
1-jet Low	31 761	180 ± 70	$31\,510 \pm 120$	1.00	0.6
1-jet Very Low	73 578	200 ± 80	$73\,330 \pm 200$	0.75	0.3
0-jet High	19 445	120 ± 50	$19\,260 \pm 90$	0.89	0.6
0-jet Medium	50 742	200 ± 80	$50\,830 \pm 190$	0.90	0.4
0-jet Low	94 032	240 ± 90	$93\,770 \pm 210$	0.78	0.3
0-jet Very Low	136 762	170 ± 60	$136\,510 \pm 290$	0.47	0.1